FINITE ELEMENT ANALYSIS FOR BUCKLING OF SEMIRIGID SPACE FRAMES

A Thesis

Presented To

the Faculty of the School of Engineering and Applied Science

University of Virginia

In Partial Fulfillment

of the Requirements for the Degree

Master of Civil Engineering

by

James Warren Ramsey, Jr.

June 1968

APPROVAL SHEET

This thesis is submitted in partial fulfillment of

the requirements for the degree of

Master of Civil Engineering

_____

Author

Approved:

_____

Faculty Advisor

_____

Dean, School of Engineering and
Applied Science

June 1968

ABSTRACT

A theory for buckling of three-dimensional space frames by finite element methods is developed. A procedure for automation of buckling calculations is presented. An accuracy study is made of the convergence of the theory by finite difference methods and applied to the pinned, fixed, and cantilever column problems. The semirigid joints are introduced by a linear spring approach. Two- and three-dimensional numerical examples are presented that show the influence of semirigid joints on buckling loads. The procedure used to solve for the buckling loads in the examples is determinant plotting. The results for the problems studied show that practical moment resisting joints may be assumed to be rigid with a slightly nonconservative buckling load. Also, it is shown that practical moment free connections have a substantial amount of residual strength for buckling.

ACKNOWLEDGMENTS

The author wishes to thank Dr. Robert E. Fulton for his guidance and constructive criticism throughout the preparation of this paper and Professor R. T. Eppink for encouragement and helpful criticism of this text. Acknowledgment is given to the National Aeronautics and Space Administration for use of the computer center and for the typing of the paper.

The author also wishes to thank his wife, Jane, for her moral support during the course of the research.

TABLE OF CONTENTS

LIST OF TABLES

LIST OF FIGURES

FIGURE PAGE

LIST OF SYMBOLS

A	cross sectional area
A_m	amplitude of sine wave
E	modulus of elasticity
e	bowing effect
G	shear modulus of elasticity
h	length of element
I	moment of inertia
J	torsional constant
K^o	conventional stiffness matrix
K'	geometric matrix
L	length of member
L_e	effective length of member
M_s	moment at semirigid joint
M	miscellaneous shapes
M_z, M_y, M_x	moments about cross section
O	order of error
P	concentrated applied load
P_{CR}	buckling load
R	stiffness of semirigid joints
T	superscript denoting transformed
U	internal potential energy
V	total potential energy
w,v	deflections of element
WF	wide flange shape

X_{EXTRAP}	linear extrapolation result
θ_x, θ_y, θ_z	rotations of element
,x	subscript denoting partial derivative
β	transformation matrix
ϕ,θ	semirigid angles
σ_x	axial stress
$\sum$	summation symbol
Ω	external potential energy

CHAPTER 1

INTRODUCTION

The buckling of planar frames has been the subject of an extensive amount of experimental and theoretical study.[1,2] A survey of these investigations[2] has led to simple formulas from which buckling loads can be calculated. Most buckling analyses assume that the joints are rigid. For real structures, however, the joints are not rigid but have some flexibility due to the method of connection (bolted or welded). Such practical joints can be termed "semirigid." If it is assumed that the joint is rigid and is actual semirigid, the buckling load will be overstated. A joint assumed to be pinned and is actually semirigid, the buckling load may be understated. A safer and more economical design would result if the effect of the semirigidity of the connections were included in analyzing a frame. Some work on the influence of semirigidity for frames has been accomplished for planar frames.[1,3,4] For instance, Goering[1] used a generalized slope deflection method with fictitious members to represent the semirigid joints. Monforton and Wu[2] modified the stiffness matrices for the members by using a correction matrix. Also, the methods used for planar studies (rigid or semirigid) do not appear to be easily extendable to three-dimensional buckling and another approach seems to be required.

An approximate method which has merit for handling three-dimensional buckling including the influence of joint flexibility is

the finite element method of structural analysis. This method is a Rayleigh-Ritz approximation as applied to the displacement shapes. It is well suited for calculation on a digital computer and has the potential of being applicable to almost unlimited cases of complicated structures composed of beams, plates or shell segments. Because of its advantages the finite element method has been chosen for use in this study.

The purpose of thes thesis is to extend the finite element method to compute buckling loads of three-dimensional structures allowing for joint flexibility. A linear spring is used to approximate the semirigidity of the connections. Torsional stiffness $\left(\frac{GJ}{h}\right)$ for any given member is provided; however, torsional semirigid joints are not considered. Twist buckling is not included in this study and limits the sample problems to frames composed of cross sections consistant with simple beam-column behavior. The derivation and a study of accuracy of the three-dimensional buckling matrices are presented, as well as sample problems for two- and three-dimensional frames having both rigid and semirigid joints. The development assumes inextensional buckling behavior for all compression members. The stiffness values used for the semirigid joints were based on the series of tests performed by Rathbun[5] on representative joints for real structures.

CHAPTER II

MATRIX ANALYSIS BY FINITE ELEMENT METHODS

2.1 Derivation of Three-Dimensional Stiffness and Geometric Matrices

In the finite element method it is customary to obtain a characterization of the stiffness properties, $[K]$, of each element and relate the end nodal displacements, $\{u\}$, to the end internal forces $\{F\}$ by

$$\{F\} = [K] \{u\} . \tag{1}$$

A symbolic finite beam element with ends at points 1 and 2 is shown in Figure 2.1.1. The vectors $\{u_1\}$ and $\{F_1\}$ are the respective vectors of

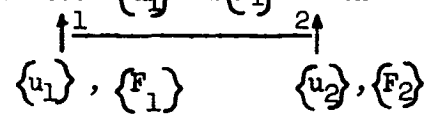

Figure 2.1.1- Finite element.

end displacements and force resultants. Thus Equation (1), as applied to Figure 2.1.1, is

$$\begin{Bmatrix} F_1 \\ F_2 \end{Bmatrix} = [K] \begin{Bmatrix} u_1 \\ u_2 \end{Bmatrix} \tag{2}$$

where $[K]$ is the stiffness matrix of the finite element. For buckling problems there are two parts to $[K]$ (ref. 6) in Equation (1), the bending stiffness portion $[K^o]$ and the portion dependant on P $[K']$. Thus, for buckling, Equation (2) can be written in the form

$$\begin{Bmatrix} F_1 \\ F_2 \end{Bmatrix} = [K^o] \begin{Bmatrix} u_1 \\ u_2 \end{Bmatrix} + [K'] \begin{Bmatrix} u_1 \\ u_2 \end{Bmatrix} . \tag{3}$$

This section contains a derivation of the $[K^o]$ and $[K']$ matrices for three-dimensional column buckling.

The sign convention for rotations used in this thesis follows the right hand rule and is shown in Figure 2.1.2. Consider a continuous prismatic beam element with a length h and a symmetrical cross section subjected to a constant axial load P. The strain energy of the beam which takes into account bending about both axes and constant torque is

$$U = \frac{1}{2}\int_0^h \left[EI_z v^2_{,xx} + EI_y w^2_{,xx} + \frac{GJ}{h^2}\theta^2_{x,x} \right] dx \qquad (4)$$

The terms EI, GJ are the bending and torsional stiffnesses and v, w, θ_x are the relative displacements of the beam element (Figure 2.1.2). The distance along the element is x and the subscript x following a comma denotes differentation with respect to x. If inextensional behavior is assumed, the bowing effect of a differential segment dx in the x-y and x-z planes of Figure 2.1.3(b) due to out of plane motion is

$$\begin{aligned} e &= dx - \left(dx^2 - dv^2 - dw^2\right)^{\frac{1}{2}} \\ e &= \left\{1 - \left[1 - \left(v^2_{,x} + w^2_{,x}\right)\right]^{\frac{1}{2}}\right\} dx \end{aligned} \qquad (5)$$

Expand the total bowing term of Equations (5) in a binomial series. The result for the segment is

$$\begin{aligned} e &= dx \left\{1 - \left[1 - \frac{1}{2}\left(v_{,x}^{\,2} + w_{,x}^{\,2}\right) + \ldots\right]\right\} \\ e &= \frac{1}{2}\left(v_{,x}^{\,2} + w_{,x}^{\,2}\right) dx \end{aligned} \qquad (6)$$

The external potential energy of the bowing effect for the element is

$$\Omega = \int_A \int_0^h e \ \sigma_x \, dA$$

where

$$\sigma_x = \frac{P}{A}$$

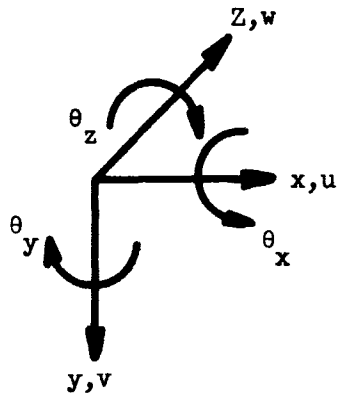

Figure 2.1.2.- Sign convention.

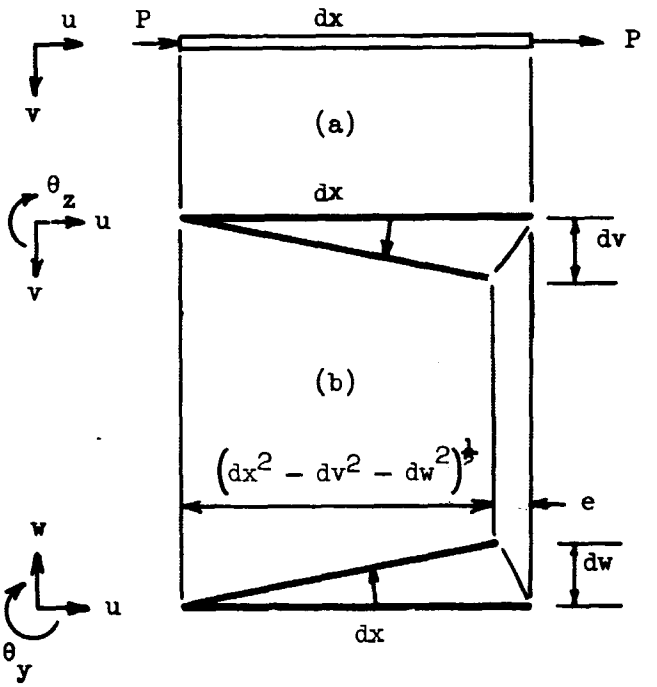

Figure 2.1.3.- Bowing effect.

Then, if the axial force and the area of the member are constant:

$$\Omega = \frac{P}{2} \int_0^h \left(v_{,x}^2 + w_{,x}^2 \right) \, dx \tag{7}$$

The total potential energy of the element is the sum of Equations (4) and (7):

$$V = \Omega + U$$

$$V = \frac{1}{2} \int_0^h \left[EI_z \, v_{,xx}^2 + EI_y \, w_{,xx}^2 + \frac{GJ}{h^2} \, \theta_{x,x}^2 + P \left(v_{,x}^2 + w_{,x}^2 \right) \right] dx \tag{8}$$

The Rayleigh-Ritz method is used to approximate the behavior of the finite element. The displacements shapes (v,w) are assumed that satisfy the boundary conditions at each end. The simplest set of approximations that satisfy the boundary conditions – the arbitrary displacements and rotations at the ends of the element – is the following:

$$\begin{aligned} \theta_x &= a_0 + a_1 x \\ v &= b_0 + b_1 x + b_2 x^2 + b_3 x^3 \\ w &= c_0 + c_1 x + c_2 x^2 + c_3 x^3 \end{aligned} \tag{9}$$

where a_i, b_i, and c_i are constants of integration. These displacement states correspond to that resulting for a prismatic beam undergoing small displacements and subjected to end loads.

It can be seen from Equation (8) and Equations (9) that the bowing effect as well as the various energies are uncoupled from each other and can be handled separately. Therefore, the bending derivation will be restricted to two dimensions to compare with Martin's work (ref. 6) and these results will be subsequently utilized to obtain the

complete three-dimensional behavior.

Solving for the constants of Equations (9) in terms of the nodal displacements of the element results in the following:

$$\theta_x = (\theta_{x_2} - \theta_{x_1})x \tag{10a}$$

$$v = v_1 + \theta_{z_1} x + \left[\frac{3}{h^2}\left(v_2 - v_1\right) - \frac{1}{h}\left(2\,\theta_{z_1} + \theta_{z_2}\right)\right]x^2 + \left[\frac{2}{h^3}\left(v_1 - v_2\right) + \frac{1}{h^2}\left(\theta_{z_1} + \theta_{z_2}\right)\right]x^3 \tag{10b}$$

$$w = w_1 - \theta_{y_1} x + \left[\frac{3}{h^2}\left(w_2 - w_1\right) + \frac{1}{h}\left(2\theta_{y_1} + \theta_{y_2}\right)\right]x^2 + \left[\frac{2}{h^3}\left(w_1 - w_2\right) - \frac{1}{h^2}\left(\theta_{y_1} + \theta_{y_2}\right)\right]x^3 \tag{10c}$$

Let V_1 be the two- dimensional portion of the potential energy and V_2 the remaining portion. Using the calculus of variations(incrementing V_1 by a virtual displacement), Equation (8), excluding $w_{,xx}$ and $w_{,x}$ terms, is

$$V_1 + \Delta V_1 = \frac{1}{2}\int_0^h \left[EI_z\left(v_{,xx} + \delta v_{,xx}\right)^2 + \frac{GJ}{h^2}\left(\theta_{x,x} + \delta\theta_{x,x}\right)^2 + P\left(v_{,x} + \delta v_{,x}\right)^2\right]dx \tag{11}$$

Expanding and grouping together those terms linear in the virtual displacement δV_1 and quadratic as $\delta^2 V_1$ yields

$$V_1 + \Delta V_1 = V_1 + \delta V_1 + \delta^2 V_1 \qquad (12)$$

From energy principles it is known that $\delta V = 0$ for equilibrium and $\delta^2 V > 0$ for stability (See ref. 7). Since the only term that is of interest in buckling is the second variation $\delta^2 V_1$, it will be evaluated. Note that for this problem the potential function is quadratic and the variations higher than the second vanish. Thus

$$\delta^2 V_1 = \frac{1}{2} \int_0^h \left\{ EI_z \, \delta^2 v_{,xx} + \frac{GJ}{h^2} \left(\delta^2 \theta_{x,x} \right) + P \, \delta^2 v_{,x} \right\} dx \qquad (13)$$

The appropriate variations of Equations (10a) and (10b) are substituted into Equation (13). The result after expansion and integration is the following:

$$\begin{aligned} \delta^2 V_1 = \frac{1}{2} \Bigg\{ & \frac{GJ}{h} \left(\delta\theta_{x_2} - \delta\theta_{x_1} \right)^2 \\ & + \left(\frac{12EI_z}{h^3} + \frac{6P}{5h} \right) \left(\delta v_2 - \delta v_1 \right)^2 - \left(\frac{12EI_z}{h^2} + \frac{P}{5} \right) \left(\delta v_2 \right. \\ & \left. - \delta v_1 \right) \left(\delta\theta_{z_1} + \delta\theta_{z_2} \right) + \left(\frac{4EI_z}{h} + \frac{2Ph}{15} \right) \left(\delta^2 \theta_{z_1} + \delta^2 \theta_{z_2} \right) \\ & + \left(\frac{4EI_z}{h} - \frac{Ph}{15} \right) \delta\theta_{z_1} \, \delta\theta_{z_2} \Bigg\} \end{aligned} \qquad (14)$$

Equation (14) can be written in matrix form as

$$\delta^2 V_1 = \frac{1}{2} \left\{ \delta u \right\}^T [K] \left\{ \delta u \right\} \qquad (15)$$

Separating K into two matrices, K^o and K' gives the following result:

$$K^o = \begin{array}{c|ccc|ccc} & \delta v_1 & \delta\theta_{x_1} & \delta\theta_{z_1} & \delta v_2 & \delta\theta_{x_2} & \delta\theta_{z_2} \\ \hline & \frac{12EI_z}{h^3} & 0 & \frac{6EI_z}{h^2} & -\frac{12EI_z}{h^3} & 0 & \frac{6EI_z}{h^2} \\ & 0 & \frac{GJ}{h} & 0 & 0 & -\frac{GJ}{h} & 0 \\ & \frac{6EI_z}{h^2} & 0 & \frac{4EI_z}{h} & -\frac{6EI_z}{h^2} & 0 & \frac{2EI_z}{h} \\ \hline & -\frac{12EI_z}{h^3} & 0 & -\frac{6EI_z}{h^2} & \frac{12EI_z}{h^3} & 0 & -\frac{6EI_z}{h^2} \\ & 0 & -\frac{GJ}{h} & 0 & 0 & \frac{GJ}{h} & 0 \\ & \frac{6EI_z}{h^2} & 0 & \frac{2EI_z}{h} & -\frac{6EI_z}{h^2} & 0 & \frac{4EI_z}{h} \end{array} \qquad (16)$$

Where the ordering of the $\{\delta u\}$ variations is shown along the top of the matrix.

$$K' = P$$

	δv_1	$\delta\theta_{x_1}$	$\delta\theta_{z_1}$	δv_2	$\delta\theta_{x_2}$	$\delta\theta_{z_2}$
	$\frac{6}{5h}$	0	$\frac{1}{10}$	$-\frac{6}{5h}$	0	$\frac{1}{10}$
	0	0	0	0	0	0
	$\frac{1}{10}$	0	$\frac{2h}{15}$	$-\frac{1}{10}$	0	$-\frac{h}{30}$
	$-\frac{6}{5h}$	0	$-\frac{1}{10}$	$\frac{6}{5h}$	0	$-\frac{1}{10}$
	0	0	0	0	0	0
	$\frac{1}{10}$	0	$-\frac{h}{30}$	$-\frac{1}{10}$	0	$\frac{2h}{15}$

(17)

Equation (16) is the standard, two-dimensional finite element stiffness matrix and Equation (17) is the two-dimensional geometric matrix reported by Martin, but derived in a different manner.[6]

To extend this in the third dimension, Equation (10c) and the remaining portion of Equation (8) are used to obtain, through the same procedures as Equations (11), (12), (13), and (14), the following additional terms to the second variation ($\delta^2 V_2$):

$$\delta^2 V_2 = \frac{1}{2}\left\{\left(\frac{12EI_y}{h^3} + \frac{6P}{5h}\right)(\delta w_2 - \delta w_1)^2 + \left(\frac{12EI_y}{h^2} + \frac{P}{5}\right)(\delta w_2 - \delta w_1)(\delta\theta_{y_1} + \delta\theta_{y_2}) + \left(\frac{4EI_y}{h} + \frac{2Ph}{15}\right)(\delta^2\theta_{y_1} + \delta^2\theta_{y_2}) + \left(\frac{4EI_y}{h} - \frac{2Ph}{30}\right)\delta\theta_{z_1}\,\delta\theta_{z_2}\right\} \tag{18}$$

It is seen in Equations (16) and (17) that there is no extensional contribution in the K^o and K' matrices. Extensional behavior is neglected in the buckling behavior of the element corresponding to the usual inextensional assumption made when deriving the differential equation for column stabily. The final three-dimensional finite element stiffness matrix K^o obtained by adding the applicable part of Equation (18) to Equation (16), is the following:

$$K^o = \begin{array}{c} \begin{matrix} \delta v_1 & \delta w_1 & \delta\theta_{x_1} & \delta\theta_{y_1} & \delta\theta_{z_1} & \delta v_2 & \delta w_2 & \delta\theta_{x_2} & \delta\theta_{y_2} & \delta\theta_{z_2} \end{matrix} \\ \left[\begin{array}{ccccc|ccccc} \frac{12EI_z}{h^3} & 0 & 0 & 0 & \frac{6EI_z}{h^2} & -\frac{12EI_z}{h^3} & 0 & 0 & 0 & \frac{6EI_z}{h^2} \\ 0 & \frac{12EI_y}{h^2} & 0 & -\frac{6EI_y}{h^2} & 0 & 0 & -\frac{12EI_y}{h^3} & 0 & -\frac{6EI_y}{h^2} & 0 \\ 0 & 0 & \frac{GJ}{h} & 0 & 0 & 0 & 0 & -\frac{GJ}{h} & 0 & 0 \\ 0 & -\frac{6EI_y}{h^2} & 0 & \frac{4EI_y}{h} & 0 & 0 & \frac{6EI_y}{h^2} & 0 & \frac{2EI_y}{h} & 0 \\ \frac{6EI_z}{h^2} & 0 & 0 & 0 & \frac{4EI_z}{h} & -\frac{6EI_z}{h^2} & 0 & 0 & 0 & \frac{2EI_z}{h} \\ \hline -\frac{12EI_z}{h^3} & 0 & 0 & 0 & -\frac{6EI_z}{h^2} & \frac{12EI_z}{h^3} & 0 & 0 & 0 & -\frac{6EI_z}{h^2} \\ 0 & -\frac{12EI_y}{h^3} & 0 & \frac{6EI_y}{h^2} & 0 & 0 & \frac{12EI_y}{h^3} & 0 & \frac{6EI_y}{h^2} & 0 \\ 0 & 0 & -\frac{GJ}{h} & 0 & 0 & 0 & 0 & \frac{GJ}{h} & 0 & 0 \\ 0 & -\frac{6EI_y}{h^2} & 0 & \frac{2EI_y}{h} & 0 & 0 & \frac{6EI_y}{h^2} & 0 & \frac{4EI_y}{h} & 0 \\ \frac{6EI_z}{h^2} & 0 & 0 & 0 & \frac{2EI_z}{h} & -\frac{6EI_z}{h^2} & 0 & 0 & 0 & \frac{4EI_z}{h} \end{array}\right] \end{array} \tag{19}$$

The final three-dimensional finite element geometric matrix K' is obtained by adding the rest of Equation (18) to Equation (17):

$$K' = P \begin{array}{c} \begin{matrix} \delta v_1 & \delta w_1 & \delta\theta_{x_1} & \delta\theta_{y_1} & \delta\theta_{z_1} & \delta v_2 & \delta w_2 & \delta\theta_{x_2} & \delta\theta_{y_2} & \delta\theta_{z_2} \end{matrix} \\ \left[\begin{array}{ccccc|ccccc} \frac{6}{5h} & 0 & 0 & 0 & \frac{1}{10} & -\frac{6}{5h} & 0 & 0 & 0 & \frac{1}{10} \\ 0 & \frac{6}{5h} & 0 & -\frac{1}{10} & 0 & 0 & -\frac{6}{5h} & 0 & -\frac{1}{10} & 0 \\ 0 & 0 & 0 & 0 & 0 & 0 & 0 & 0 & 0 & 0 \\ 0 & -\frac{1}{10} & 0 & \frac{2h}{15} & 0 & 0 & \frac{1}{10} & 0 & -\frac{h}{30} & 0 \\ \frac{1}{10} & 0 & 0 & 0 & \frac{2h}{15} & -\frac{1}{10} & 0 & 0 & 0 & -\frac{h}{30} \\ \hline -\frac{6}{5h} & 0 & 0 & 0 & -\frac{1}{10} & \frac{6}{5h} & 0 & 0 & 0 & -\frac{1}{10} \\ 0 & -\frac{6}{5h} & 0 & \frac{1}{10} & 0 & 0 & \frac{6}{5h} & 0 & \frac{1}{10} & 0 \\ 0 & 0 & 0 & 0 & 0 & 0 & 0 & 0 & 0 & 0 \\ 0 & -\frac{1}{10} & 0 & -\frac{h}{30} & 0 & 0 & \frac{1}{10} & 0 & \frac{2h}{15} & 0 \\ \frac{1}{10} & 0 & 0 & 0 & -\frac{h}{30} & -\frac{1}{10} & 0 & 0 & 0 & \frac{2h}{15} \end{array}\right] \end{array} \tag{20}$$

The equilibrium equations describing the end forces $\{F\}$ in terms of any set of nodal displacements (virtual or real) is

$$\{F\} = [K^o + K']\{u\} \tag{21}$$

where

$$\{u\} = \begin{Bmatrix} v_1 \\ w_1 \\ \theta_{x_1} \\ \theta_{y_1} \\ \theta_{z_1} \\ v_2 \\ w_2 \\ \theta_{x_2} \\ \theta_{y_2} \\ \theta_{z_2} \end{Bmatrix}; \{F\} = \begin{Bmatrix} P_{y_1} \\ P_{z_1} \\ M_{x_1} \\ M_{y_1} \\ M_{z_1} \\ P_{y_2} \\ P_{z_2} \\ M_{x_2} \\ M_{y_2} \\ M_{z_2} \end{Bmatrix} \tag{22}$$

2.2 Introduction of Semirigid Joints

In this study the influence of semirigidity will be studied. Some method of introducing joint flexibility must be provided. The method selected is the use of a linear spring between members at a joint. The strain energy of the spring is

$$U_s = \int_0^{\theta} M_s d\theta \quad \text{where} \quad M_s = R\theta$$

$$U_s = \int_0^{\theta} R\theta \, d\theta \tag{23}$$

$$U_s = \frac{R\theta^2}{2}$$

Where R is the spring or joint stiffness.

Some typical examples of this approach for semirigidity are shown in Figures 2.2.1 and 2.2.2. In all cases the column angle is used as the base angle (datum plane) for determining the slippage of the joint. A typical deformed joint is shown in Figure 2.2.1(a).

The total strain energies for the two-dimensional springs of Figure 2.2.1 (a) and (b), respectively, are as follows:

$$U_s = \frac{R_1}{2}\left(\theta_1 - \theta_2\right)^2 \tag{24a}$$

$$\sum U_s = \frac{R_2}{2}\left(\theta_3 - \theta_4\right)^2 + \frac{R_3}{2}\left(\theta_3 - \theta_5\right)^2 \tag{24b}$$

The total strain energies for the same joints but adding the third-dimensional member, Figure 2.2.2(a) and (b), respectively, are as follows:

$$\sum U_s = \frac{R_4}{2}\left(\theta_6 - \theta_7\right)^2 + \frac{R_5}{2}\left(\theta_6 - \phi_1\right)^2 \tag{25a}$$

$$\sum U_s = \frac{R_6}{2}\left(\theta_8 - \theta_9\right)^2 + \frac{R_7}{2}\left(\theta_8 - \theta_{10}\right)^2 + \frac{R_8}{2}\left(\theta_8 - \phi_2\right)^2 \tag{25b}$$

For example, the matrix format of the second variation terms that come from Equation (24a) is

$$\left[R^s\right]\{u\} = \begin{bmatrix} \delta\theta_1 & \delta\theta_2 \\ R_1 & -R_1 \\ -R_1 & R_1 \end{bmatrix} \begin{Bmatrix} \delta\theta_1 \\ \delta\theta_2 \end{Bmatrix} \tag{26}$$

where $\left[R^s\right]$ is the spring stiffness matrix for the joint of Figure 2.2.1(a).

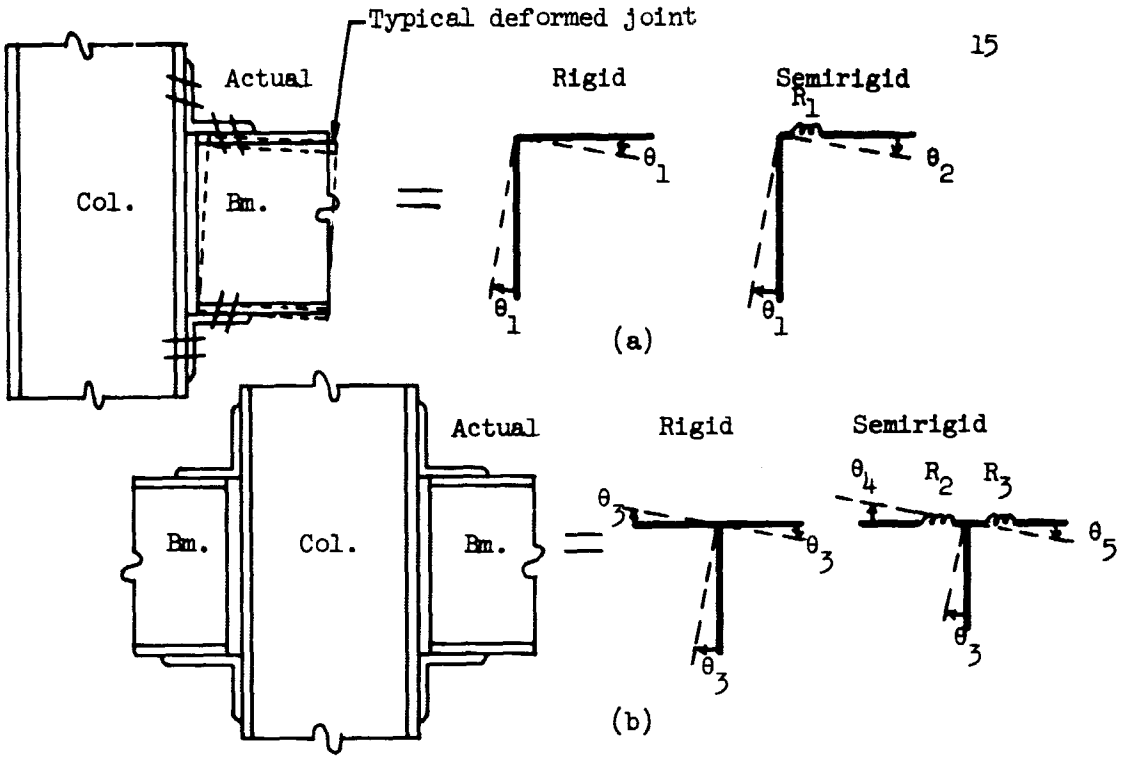

Figure 2.2.1.- Two-dimensional joints.

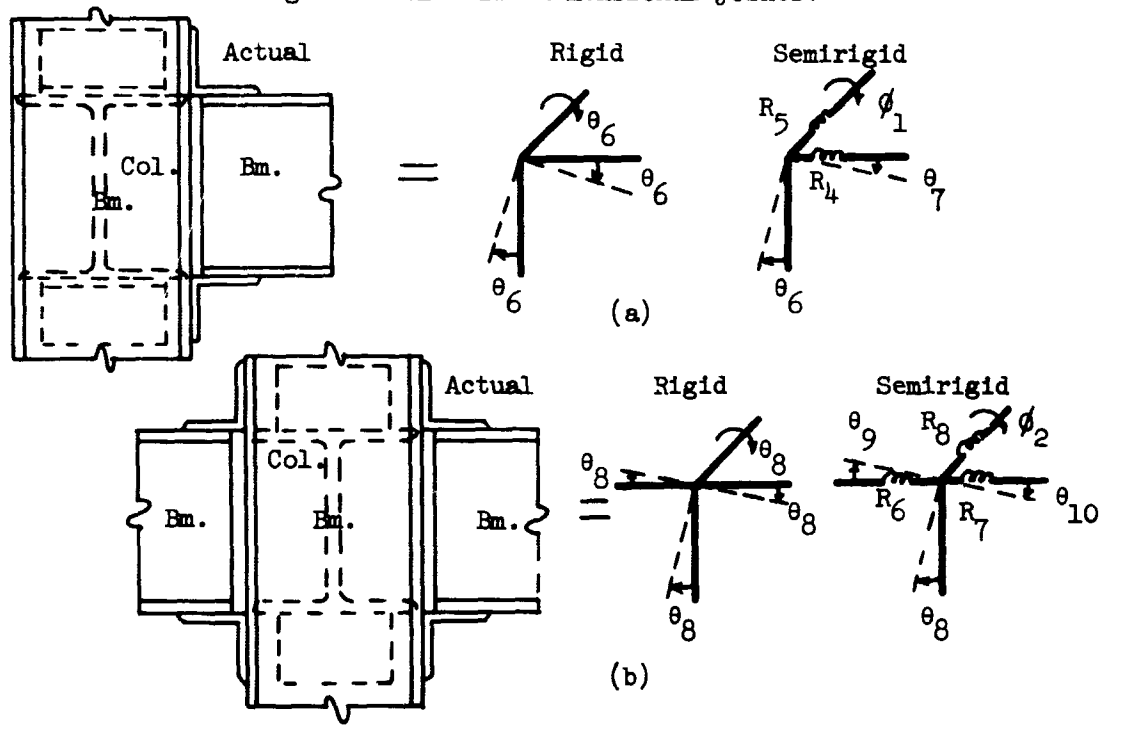

Figure 2.2.2.- Three-dimensional joints.

The semirigid connection may be thought of as a locally weakened section between the end of a beam and the face of the column to which the connection is made. Reference (1) points out that only a small part of the rotation of a semirigid joint is due to bending of the angles. Most of the rotation is due to slip and extension of its rivets or bolts. Since this semirigid joint is quite complex and involves other types of movement such as local bending of the column, this thesis will be concerned only with the use of a linear rotational spring to represent the semirigid joint.

The rotational springs of the column and beam have additional nodal stiffnesses, $\left(\frac{4EI}{h}\right)_{\text{column}}$ and $\left(\frac{4EI}{h}\right)_{\text{beam}}$. The rigid joint stiffness form can be expressed as the following:

$$\begin{matrix} & (\delta\theta_1)_{\text{column}} + (\delta\theta_1)_{\text{beam}} \\ K = \Bigg[& \frac{4EI}{h}_{\text{column}} + \frac{4EI}{h}_{\text{beam}} \Bigg] \end{matrix} \qquad (27)$$

Equation (27) must be included in Equation (26) to obtain the complete semirigid stiffness of the joint. The result is

$$\begin{matrix} & & \delta\theta_1 & & \delta\theta_2 & \\ [\bar{K}]\{u\} = \Bigg[& \delta\theta_1 & \frac{4EI}{h}_{\text{column}} + R_1 & & -R_1 & \Bigg] \Bigg\{ \begin{matrix} \delta\theta_1 \\ \delta\theta_2 \end{matrix} \Bigg\} \\ & \delta\theta_2 & -R_1 & & \frac{4EI}{h}_{\text{beam}} + R_1 & \end{matrix} \qquad (28)$$

where $[\bar{K}]$ is the semirigid joint stiffness matrix of Figure 2.2.1(a).

2.3 Automated Technique of Matrix Methods

2.3.1 Procedure for stress analysis. The process for generating a computer program of any structure that is composed of many finite elements is to first pick a set of coordinates convenient for a typical element. The generalized element displacements are $\{\delta\}$ and forces are $\{P\}$. The energy in terms of element coordinates is

$$U = \frac{1}{2} \{\delta\}^T [K] \{\delta\} \tag{29}$$

The displacements $\{\delta\}$ and stiffness matrix $[K]$ are partitioned corresponding to ends i and j

$$[K] \{\delta\} = \{P\} \tag{30}$$

$$\begin{bmatrix} K_{ii} & K_{ij} \\ K_{ji} & K_{jj} \end{bmatrix} \begin{Bmatrix} \delta_i \\ \delta_j \end{Bmatrix} = \begin{Bmatrix} P_i \\ P_j \end{Bmatrix} \tag{31}$$

In the process of connecting elements, it is found that one element's local coordinates are not the same for another element. Therefore, a set of system coordinates is chosen that is convenient for a system of elements and the local coordinate points are numbered (points 1, 2, 3, ...).

A systematic numbering process for the node points and members

is chosen. The element properties (E, A, I, L) are given. The stiffness K_{ij} for each element is calculated in local coordinates where i and j refer to the end points of each element.

If the system coordinates are called $\{u\}$, the transformation from an element's coordinates to a system's coordinates is accomplished by a transformation matrix, $[\beta]$. [8] That is

$$\{\delta\} = [\beta]\{u\} \tag{32}$$

The stiffness of the element is transformed to system coordinates by Equation (32).

$$[\bar{K}] = [\beta]^T [K] [\beta] \tag{33}$$

Consider several elements that are connected. The next step is to generate the master stiffness matrix $[K_{ij}]_M$ by summing all member stiffnesses. It can be shown that the elements of $[K_{ij}]_M$ can be obtained as follows:

$$[K_{ij}]_M = \sum_{\substack{\text{All} \\ \text{members}}} [\bar{K}_{ij}] \tag{34}$$

For all displacements that are constrained(boundary conditions), it can also be shown that this can be handled by striking out rows and columns corresponding to the displacement constraints, resulting in the reduced master stiffness matrix $[K]_R$.

Finally, the system applied external forces $\{Q\}$ are identified and the equation

$$[K]_R \{u\}_R = \{Q\}_R \tag{35}$$

is solved.

2.3.2 Buckling procedure. For the buckling

problem the steps are essentially the same as for the preceding section except that the stiffness matrix K for an element is composed of two parts, K^{o}, the stiffness of the structure and K', which contains P – the eigenvalue portion of the problem. The remaining steps are the same with the external concentrated axial loads at the joints equal to the internal forces of the column elements in the K' matrix. Since the external lateral forces and moments at the junction of the beam elements are equal to zero in all cases studied in this thesis, the equilibrium equation for inextensional behavior is

$$\left[K^{o}_{R} + K'_{R}\right]\{u\} = 0. \tag{36}$$

A nontrivial solution to equation (36) requires that the determinant

$$\left|K^{o}_{R} + K'_{R}\right| = 0. \tag{37}$$

A similar condition results for stability based on the second variation of the potential energy of the structure. This is then solved by some standard procedure for determining eigenvalues such as determinant plotting, matrix iteration, or other procedures. The method used in this study is determinant plotting.

When the eigenvalue has been computed, the mode shape or eigenvector is obtained by assuming a value for one of the components of the eigenvector and solving for the remaining components in terms of it.

2.3.3 Semirigid joints. The process of allowing for joint flexibility adds only one additional step from that described in the previous sections. After transforming the element coordinates into system coordinates, the next step is to add the system spring stiffness matrix $\left[R^s_{ij}\right]$ similar to that in Equation (26)

$$\left[R^s_{ij}\right] = \begin{bmatrix} R_{ii} & -R_{ij} \\ -R_{ji} & R_{jj} \end{bmatrix} \tag{38}$$

to the transformed element matrix or matrices. For instance, if a semirigid joint occurs between points i and j, the resulting stiffness matrix is

$$\left[\overline{K}_{ij}\right] = \left[\overline{K}_{ij} + R^s_{ij}\right] \tag{39}$$

Any combination of Sections 2.3.1, 2.3.2 and this section can be used to give values (two- or three-dimensions) for stresses, displacements, eigenvalues, or eigenvectors either by allowing for joint flexibility or by using rigid joints.

CHAPTER III

STUDY OF CONVERGENCE

3.1 Introduction

Since the finite element method is an approximate numerical solution to structural problems, some knowledge of its reliability in these applications is desirable. This section gives the results of an investigation of the convergence and accuracy of the finite element matrices derived in Chapter II. The results are limited to simple planar buckling; however, they provide a basis for extending the methods to more complicated problems. There are many ways to study convergence and accuracy, most of which are based on numerical solutions to special problems. The approach used here is that of classical order of error analysis procedures borrowed from finite difference methods;[9] that is, to expand the discrete equations in a Taylor series about the i^{th} point.

3.2 Order of Error Analysis for $K^{\circ} + K'$

Consider a continuous prismatic beam element of length h subjected to a constant axial load P (Fig. 3.2.1). The generalized displacements are taken to be rotation θ and deflection v at the end of the element.

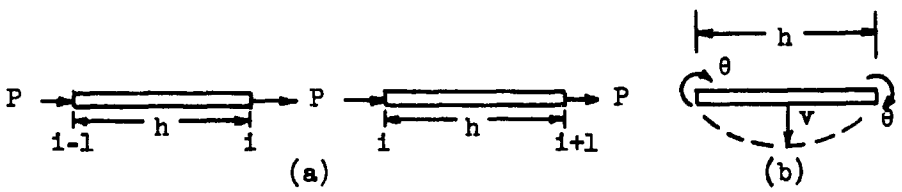

Figure 3.2.1.- Beam element.

Since the out-of-plane displacements and rotations are uncoupled from the in-plane displacements, it allows for separation of the two and only in-plane behavior will be considered to evaluate buckling reliability.

If two elements are joined together at the i^{th} point, two finite element equations result from the sum of forces and moments at the point. They are respectively,

$$\left(\frac{12EI}{h^3} + \frac{6P}{5h}\right)\left(-v_{i-1} + 2v_i - v_{i+1}\right) + \left(\frac{6EI}{h^2} + \frac{P}{10}\right)\left(-\theta_{i-1} + \theta_{i+1}\right) = 0 \tag{40}$$

and

$$\left(\frac{6EI}{h^2} + \frac{P}{10}\right)\left(v_{i-1} - v_{i+1}\right) + \left(\frac{2EI}{h} - \frac{Ph}{30}\right)\left(\theta_{i-1} + \theta_{i+1}\right) + \left(\frac{8EI}{h} + \frac{8Ph}{30}\right)\theta_i = 0 \tag{41}$$

To study the convergence character, the terms in these equations are expanded about the i^{th} point by using Taylor series such as

$$v_{i\pm1} = v_i \pm hv_i' + \frac{h^2}{2!}v_i'' \pm \cdots,$$

This leads to

$$\left(\frac{12EI}{h^3} + \frac{6P}{5h}\right)\left(-h^2 v_i'' - \frac{h^4}{12}v_i^{IV} - \frac{h^6}{360}v_i^{VI} - \frac{h^8}{56(360)}v_i^{VIII} - \cdots\right) + \left(\frac{6EI}{h^2} + \frac{P}{10}\right)\left(2h\theta_i' + \frac{h^3}{3}\theta_i''' - \frac{h^5}{60}\theta_i^{V} + \frac{h^7}{360(7)}\theta_i^{VII} + \cdots\right) = 0 \tag{42}$$

and

$$\left(\frac{6EI}{h^2} + \frac{P}{10}\right)\left(-2hv_i' - \frac{h^3}{3}v_i''' - \frac{h^5}{60}v_i^V - \frac{h^7}{360(7)}v_i^{VII}\right)$$

$$+\left(\frac{2EI}{h} - \frac{Ph}{30}\right)\left(2\theta_i + h^2\theta_i'' + \frac{h^4}{12}\theta_i^{IV} + \frac{h^6}{360}\theta_i^{VI} + \frac{h^8}{360(56)}\theta_i^{VIII}\right)$$

$$+\left(\frac{8EI}{h} + \frac{8Ph}{30}\right)\theta_i = 0 \qquad (43)$$

Since θ_i is not an independent variable in the continuum sense it is useful to eliminate it from Equation (42) and (43). By solving Equation (43) for θ_i, obtaining the successive derivatives and substituting these derivatives back into Equation (43), it becomes

$$\theta_i - v_i' + h^4\left[\frac{v_i^V}{180} - \frac{Pv_i'''}{180EI}\right] + O\left(h^6\right) = 0 \qquad (44)$$

Substituting the derivatives of θ_i into Equation (42) leads to

$$v_i^{IV} - \frac{Pv_i''}{EI} + h^4\left[-\frac{v_i^{VIII}}{720} + \frac{P}{360EI}v_i^{VI}\right] + O\left(h^6\right) = 0 \qquad (45)$$

Equations (44) and (45) show the convergence character of the finite element Equations (40) and (41) and show that they converge to

$$\theta_i - v_i' = 0 \qquad (44a)$$

and

$$v_i^{IV} - \frac{Pv_i''}{EI} = 0 \qquad (45a)$$

with both equations having an error of order h^4.

3.3 Order of Error Analysis for K^{o} - K' for String

Reference (6) suggests that a simpler method be used to obtain K' by the superposition of a string and a beam without any interaction between the two. This combination then leads to the same result of K^{o} previously derived but a modified K'. The K' for the string as applied to the planar column is

$$\begin{array}{c} \\ \frac{P}{h} \end{array} \begin{array}{c} \begin{array}{cccc} \delta v_1 & \delta\theta_1 & \delta v_2 & \delta\theta_2 \end{array} \\ \begin{bmatrix} 1 & 0 & -1 & 0 \\ 0 & 0 & 0 & 0 \\ -1 & 0 & 1 & 0 \\ 0 & 0 & 0 & 0 \end{bmatrix} \end{array} \tag{46}$$

By applying the same procedure as before, the two finite element equations at the i^{th} point are

$$\begin{aligned} &\left(\frac{12EI}{h^3} + \frac{P}{h}\right)\left(- v_{i-1} + 2v_i - v_{i+1}\right) + \frac{6EI}{h^2}\left(- \theta_{i-1} + \theta_{i+1}\right) = 0 \\ &\left(\frac{6EI}{h^2}\right)\left(- v_{i+1} + v_{i-1}\right) + \frac{2EI}{h}\left(\theta_{i-1} + 4\theta_i + \theta_{i+1}\right) = 0 \end{aligned} \tag{47}$$

Expanding as before results in

$$\begin{aligned} &\left(\frac{12EI}{h^3} + \frac{P}{h}\right)\left(- h^2 v_i'' - \frac{h^4}{12} v_i^{IV} - \frac{h^6}{360} v_i^{VI} - \frac{h^8}{360(56)} v_i^{VIII}\right) \\ &+ \left(\frac{6EI}{h^2}\right)\left(2h\,\theta_i' + \frac{h^3}{3}\theta_i''' + \frac{h^5}{60}\theta_i^{V} + \frac{h^7}{7(360)}\theta_i^{VII}\right) = 0 \end{aligned} \tag{48}$$

and

$$\frac{6EI}{h^2}\left(-2h\,v_i' - \frac{h^3}{3}v_i''' - \frac{h^5}{60}v_i^V - \frac{h^7}{2520}v_i^{VII}\right)$$

$$+\frac{2EI}{h}\left(6\theta_i + h^2\theta_i'' + \frac{h^4}{12}\theta_i^{IV} + \frac{h^6}{360}\theta_i^{VI} + \frac{h^8}{360(56)}\theta_i^{VIII}\right) = 0 \tag{49}$$

Solving Equation (49) for θ_i and substituting successive derivatives back into this equation leads to

$$\theta_i - v_i' + \frac{h^4}{180}v_i^V + \frac{h^6 v_i^{VIII}}{42(36)} = 0 \tag{50}$$

Substituting the derivatives of θ_i into Equation (48) and collecting terms gives

$$v_i^{IV} - \frac{Pv_i''}{EI} + h^2\left[-\frac{Pv_i^{IV}}{12EI}\right] + h^4\left[-\frac{v_i^{VIII}}{720} - \frac{Pv_i^{VI}}{360EI}\right] + O(h^6) = 0 \tag{51}$$

Equations (50) and (51) show that the string approximation converges to the required continuum equations but Equation (51) has $O(h^2)$. Thus its expected accuracy is less than that given in the previous section.

3.4 Application of Order of Error for $K^o + K'$

The results on order of error can be applied to obtain some further information on the accuracy of the discrete approximations in a particular set of problems.[10,11] Consider a pinned column with effective length, L_e, and subjected to a constant axial load, P.

If only the first order of error term is retained, the differential equation representing the finite element equation is

$$v_i^{IV} - \lambda_i v_i'' + h^4 \left[C_1 v_i^{VIII} + C_2 \lambda_i v_i^{VI} \right] = 0 \qquad (52)$$

where

$$\lambda_i = \frac{P}{EI}$$

The constants C_1 and C_2 taken from Equation (45) have values of $-\frac{1}{720}$ and $\frac{1}{360}$, respectively. Since h^4 is small, Equation (52) can be solved utilizing the perturbation procedure in references (10) and (11). Let

$$\lambda_i = \lambda_0 + h^4 \lambda_1 \qquad (53)$$

Where λ_1 corresponds to the order of error term.

Substituting (53) into (52) yields (retaining up to h^4 terms)

$$\left[v_i^{IV} - \lambda_0 v_i'' \right] + h^4 \left[C_1 v_i^{VIII} + C_2 \lambda_0 v_i^{VI} - \lambda_1 v_i'' \right] = 0 \qquad (54)$$

Assume

$$v_i = A_m \sin\left(\frac{m\pi x}{L_e}\right) \qquad (55)$$

The first part of Equation (54) becomes

$$A_m \left[\left(\frac{m\pi}{L_e}\right)^4 + \lambda_0 \left(\frac{m\pi}{L_e}\right)^2 \right] \sin\left(\frac{m\pi x}{L_e}\right) \qquad (56a)$$

and this must be zero independent of h^4 terms, thus

$$\lambda_0 = -\left(\frac{m\pi}{L_e}\right)^2 \qquad (56b)$$

Let

$$\bar{\lambda} = \lambda L_e^2 = \frac{PL_e^2}{EI}$$

$$\bar{\lambda}_0 = -(m\pi)^2 \tag{57}$$

The second part of Equation (54) becomes

$$A_m \left[-\frac{1}{720}\left(\frac{m\pi}{L_e}\right)^8 - \frac{1}{360}\lambda_0\left(\frac{m\pi}{L_e}\right)^6 + \lambda_1\left(\frac{m\pi}{L_e}\right)^2 \right] \sin\left(\frac{m\pi x}{L_e}\right) = 0$$

Therefore (58)

$$\bar{\lambda}_1 = -\frac{(m\pi)^2}{720}\left(\frac{m\pi}{L_e}\right)^4$$

and

$$\bar{\lambda}_i = -(m\pi)^2\left[1 + \left(\frac{h}{L_e}\right)^4 \frac{(m\pi)^4}{720}\right]$$

or (59)

$$P_{CR.} = -(m\pi)^2\left[1 + \left(\frac{h}{L_e}\right)^4 \frac{(m\pi)^4}{720}\right]\frac{EI}{L_e^2}$$

Now let N equal the number of elements per half wave, this is

$$N = \frac{L_e}{h/m}$$

The final equation form is

$$P_{CR.} = -(m\pi)^2\left[1 + \frac{1}{N^4}\frac{\pi^4}{720}\right]\frac{EI}{L_e^2} \tag{60}$$

Where the negative sign says that for buckling the member must be in compression. This shows that the error in a buckling load calculation is determined by the contribution of the principal error term ϵ, where $\epsilon = \frac{\pi^4}{N^4 720}$. Representative values of ϵ for various number of elements are as follows:

ϵ	N
20%	0.91
10%	1.08
1%	1.92

(61)

Then, two elements per buckling half wave gives the buckling load to about 1% error.

3.5 Application of Order of Error for $K^o + K'$ for String

The same procedure as the previous section is used with order of error h^2. The differential equation of the column effect approximated by a string is

$$v_i^{IV} - \lambda_i v_i'' + h^2 \left[C_1 \lambda_i v_i^{IV} \right] = 0 \qquad (62)$$

where

$$\lambda_i = \lambda_0 + h^2 \lambda_1$$

The constant $C_1 = -\frac{1}{12}$ from Equation (51) and Eq. (62) becomes

$$\left[v_i^{IV} - \lambda_0 v_i'' \right] + h^2 \left[C_1 \lambda_0 v_i^{IV} - \lambda_1 v_i'' \right] = 0 \qquad (63)$$

Solving this in the same manner as before

$$P_{CR.} = -(m\pi)^2 \left[1 + \frac{1}{N^2} \frac{\pi^2}{12} \right] \frac{EI}{L_e^2} \qquad (64)$$

The principal error term $\epsilon = \frac{\pi^2}{N^2 12}$, for various number of elements are as follows:

ϵ	N
20%	2.03
10%	2.87
1%	8.72

Thus nine elements per buckling half wave are required to obtain the buckling load to about 1% error.

3.6 Numerical Comparison

To complete the study of convergence, numerical results for the classical columns (pinned, fixed, and cantilever) were obtained for several numbers of finite element segments per column.

The results for Figures 3.6.1, 3.6.2, and 3.6.3 were obtained by the $O(h^4)$ finite element approximations ($K^o + K'$) and shown in Table 3.6.1 (a). If it is assumed that the numerical solution for $P_{CR.}$ approaches the exact solution according to the order of error, the exact result can be extrapolated by assuming a linear relation[12] for order of error $(h/L)^4$. Also, the perturbation solution to the finite element equation can be applied to simple problems. It is given in Chapter 3, Equation (60) and gives higher but reliable estimates for the results given in Table 3.6.1 (a). The perturbation results were obtained by solving Equation (60).

Results were also obtained for the $K^o + K'$ for string, $O(h^2)$ for the case of a pinned column. As an example, the data is given in Table 3.6.2 and plotted in Figure 3.6.4. The numerical data in Table 3.6.2 also shows a close comparison between the $O(h^2)$ numerical

Col. end	$P_{CR.}\ L^2/EI$					
	Number of elements				$(h/L)^4$ X_{EXTRAP}	Exact
	1	2	3	4		
Pinned	12.0000	9.9200	9.8847	—	9.8760	9.8696
Fixed	—	40.0000	40.3432	39.7754	39.5126	39.4784
Cant.	2.5000	2.4855	2.4711	—	2.4676	2.4674

(a) Numerical calculations

Col. end	$P_{CR.}\ L^2/EI$				
	Number of elements				Exact
	1	2	3	4	
Pinned	11.2049	9.9531	9.8861	—	9.8696
Cant.	2.8012	2.4883	2.4715	—	2.4674
Fixed	—	44.8194	40.5334	39.8122	39.4784

(b) Perturbation solution estimates

TABLE 3.6.1.- NONDIMENSIONAL BUCKLING LOADS, $Q(h^4)$ FOR K'

Pinned col.	$P_{CR.}\ L^2/EI$			
	Number of elements			Exact
	2	3	4	
Num.	12.0000	10.8000	10.3866	9.8696
Pert. Est.	11.8990	10.7715	10.3769	9.8696

TABLE 3.6.2.- NONDIMENSIONAL BUCKLING LOADS OBTAINED FROM "STRING" APPROXIMATION TO $K^1 - O(h^2)$

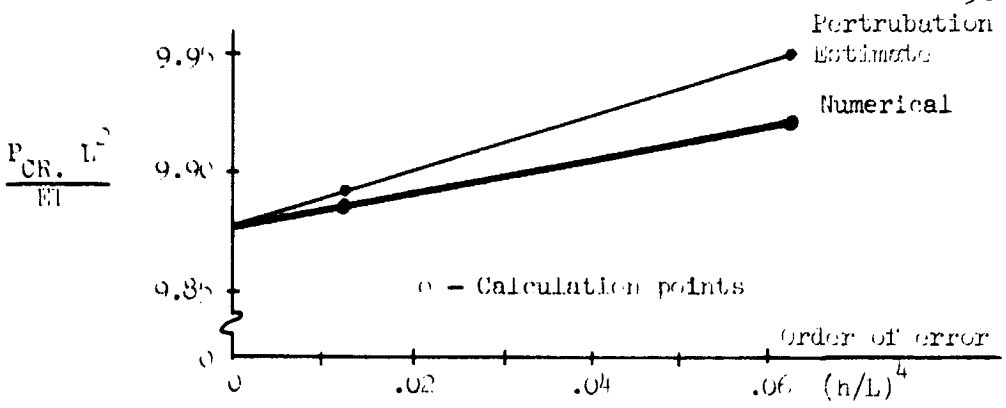

Figure 3.6.1.- Buckling loads for pinned column, $K^o + K'$.

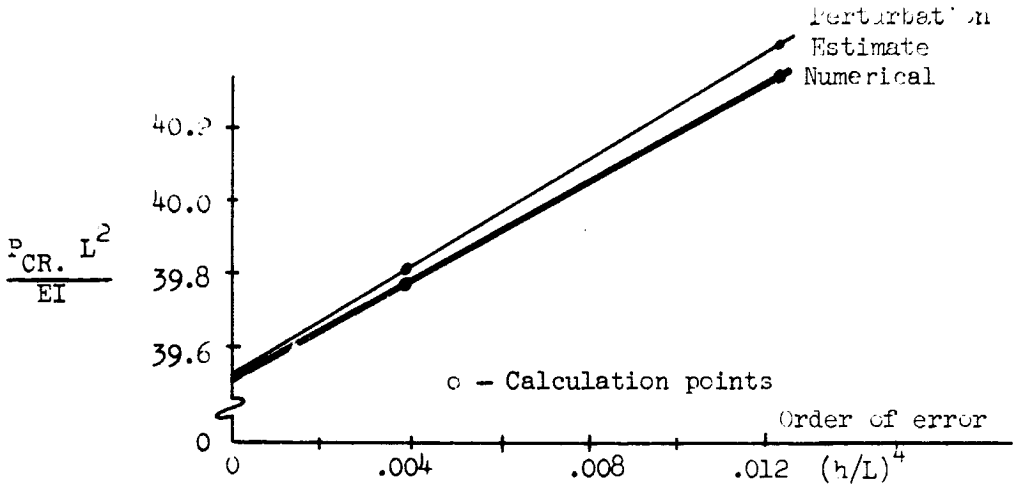

Figure 3.6.2.- Buckling loads for fixed column, $K^o + K'$.

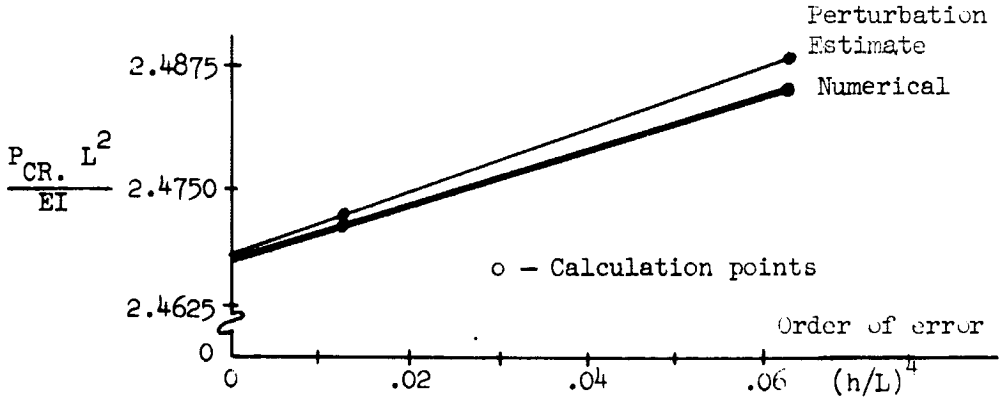

Figure 3.6.3.- Buckling loads for cantilever column, $K^o + K'$.

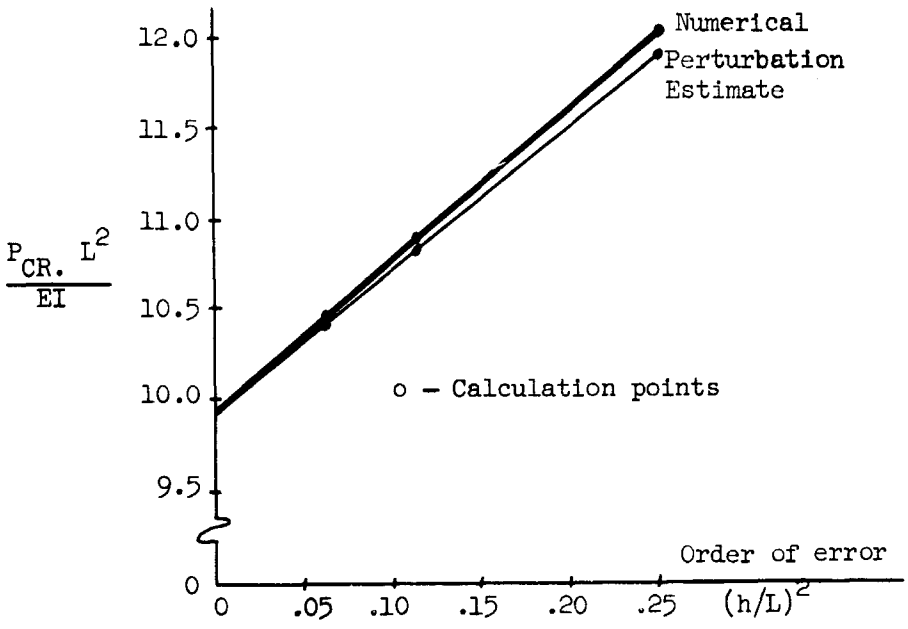

Figure 3.6.4.- Buckling loads for pinned column, $K^o + K'$ for string.

results and the perturbation estimates of the numerical results. They also demonstrate that the string finite element does have an order of error of h^2. Therefore, from a practical point of view of seeking the greatest accuracy from the least amount of work, it is obviously advantageous to use $K^o + K'$ matrices having $O(h^4)$ in lieu of the $K^o + K'$ for the string having $O(h^2)$.

The results also show that the $O(h^4)$ approximation gives good accuracy and has excellent convergence properties. The $O(h^4)$ approximation results were high but were converging to the correct answer as the number of finite elements was increased. The finite element approximation is used in the remaining portion of the study to obtain calculations for frame buckling with and without joint flexibility.

CHAPTER IV

PRESENTATION OF NUMERICAL RESULTS

4.1 Introduction

The homogeneous linear equations expressed by Equation (36) have a trivial solution, that is all displacements equal zero, and a non-trivial or unique solution where the determinant of the $[K^{\circ} + K']$ matrix equals zero. Since the trivial solution is useless, the unique solution is the one of interest here. By holding all values in the K° and K' matrices fixed, the only parameter is the axial load, P. The procedure used in this paper to determine the buckling load is to obtain the lowest nonzero value of P (load) that causes the determinant to vanish. This is accomplished by plotting the determinant versus the magnitude of the load. The numerical results were calculated using the Control Data 6600 digital computer at the Langley Research Center. Since the results are obtained for three- dimensional frame structures, several types of member properties are required. To give realistic results, specific dimensions were selected for the representative structure. The columns are all taken as 8M34.3 steel members and the beams as standard AISC 8WF31 sections. Table 4.2.1 shows the properties of these members.

4.2 Rigid Joints

Several calculations were obtained for the frames of Figure 4.2.1, where the joints were assumed to be rigid. The first

Member	Type	Big I in^4	Small I in^4	J in^4	Length ft	E psi	G psi
Columns	8M34.3	115.5	35.1	0.72	24.0	30.0 $\times 10^6$	11.2 $\times 10^6$
Beams	8WF 31	109.7	37.0	0.54	30.0		

TABLE 4.2.1.- MEMBER PROPERTIES

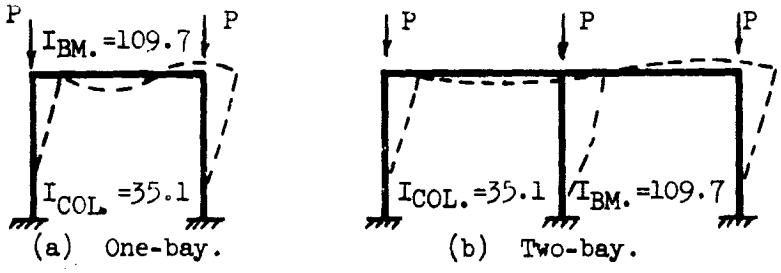

Figure 4.2.1.- Two-dimensional frames.

Frame, Finite Elememt	$P_{CR.}$, Lb.		
	$K^o + K'$	Literature	% Diff.
One-bay,one	111380	110280	+1.01
Two-bay,one	112300	111110	+1.08
Two-bay,two	111700	111110	+0.54

TABLE 4.2.2.- BUCKLING LOADS FOR TWO-DIMENSIONAL FRAMES

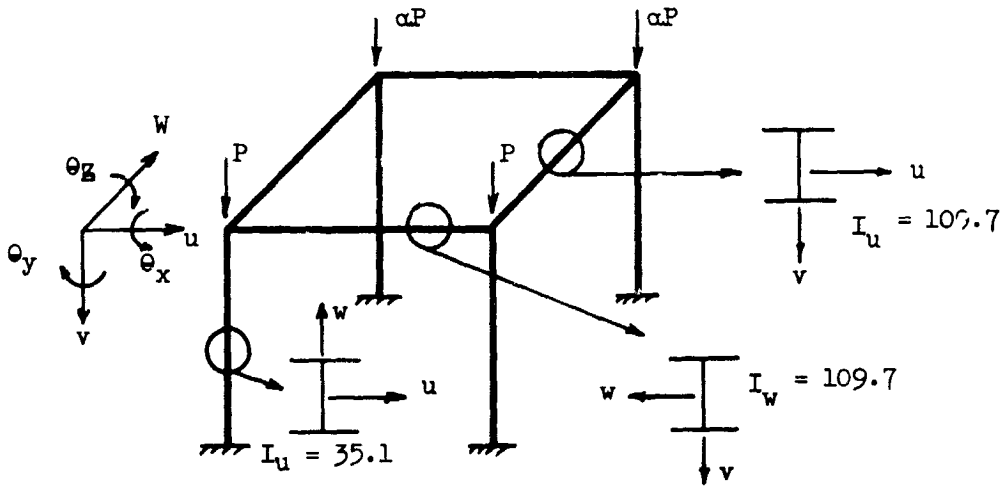

Figure 4.2.2.- Three-dimensional, one-bay frame.

results are for the case when the frames buckled as planar structures. These results were computed to compare with existing or known results (1,2) as well as to provide check points for the three-dimensional results. The comparison is shown in Table 4.2.2. For these buckling loads, the associated sidesway buckling mode shapes are indicated by a dotted line in Figure 4.2.1.

The frame of Figure 4.2.2 together with the indicated loading is used as the typical example of the three-dimensional finite element buckling theory. For various values of ALPHA (α), buckling loads were calculated, Table 4.2.3. Calculations were made for the case where the columns and beams were approximated by both one and two elements. Using these results, the graph of $P_{CR.}$ versus ALPHA, Figure 4.2.3, was obtained. Curve I shows results for a one element approximation where the columns were not allowed to twist (column GJ = ∞). Curves II and III are results for one and two element approximations to the three-dimensional structure where the columns were allowed to twist.

The eigenvector values (Curve III), using the procedure described in Chapter II are given in Table 4.2.4. With these values, the mode shapes for α = 0.0, 0.5, and 1.0 are shown in Figures 4.2.4 (a), (b), (c), (d), (e), and (f). These mode shapes are typical examples of those obtained for the problems. The mode shapes have been normalized so that the u displacements of node 1 are unity. Also, the following displacements are assumed to be equal (inextensional behavior):

$u_2 = u_{1B} = u_1$; $u_4 = u_{3B} = u_3$; $w_3 = w_{3C} = w_1$; and $w_4 = w_{2C} = w_2$.

Alpha α	$P_{CR.}$ (Lb)		
	I without torsion one element	II with torsion one element	III with torsion two elements
0.0	166900	138980	138140
0.1	162600	137840	137040
0.2	157800	136560	135760
0.3	152600	135060	134300
0.4	147000	133300	132560
0.5	141200	131180	130480
0.6	135100	128580	127900
0.7	129000	125360	124740
0.8	123000	121420	120820
0.9	117000	116720	116160
1.0	113000	111380	110840

TABLE 4.2.3.- BUCKLING LOADS FOR THREE-DIMENSIONAL, ONE-BAY FRAME

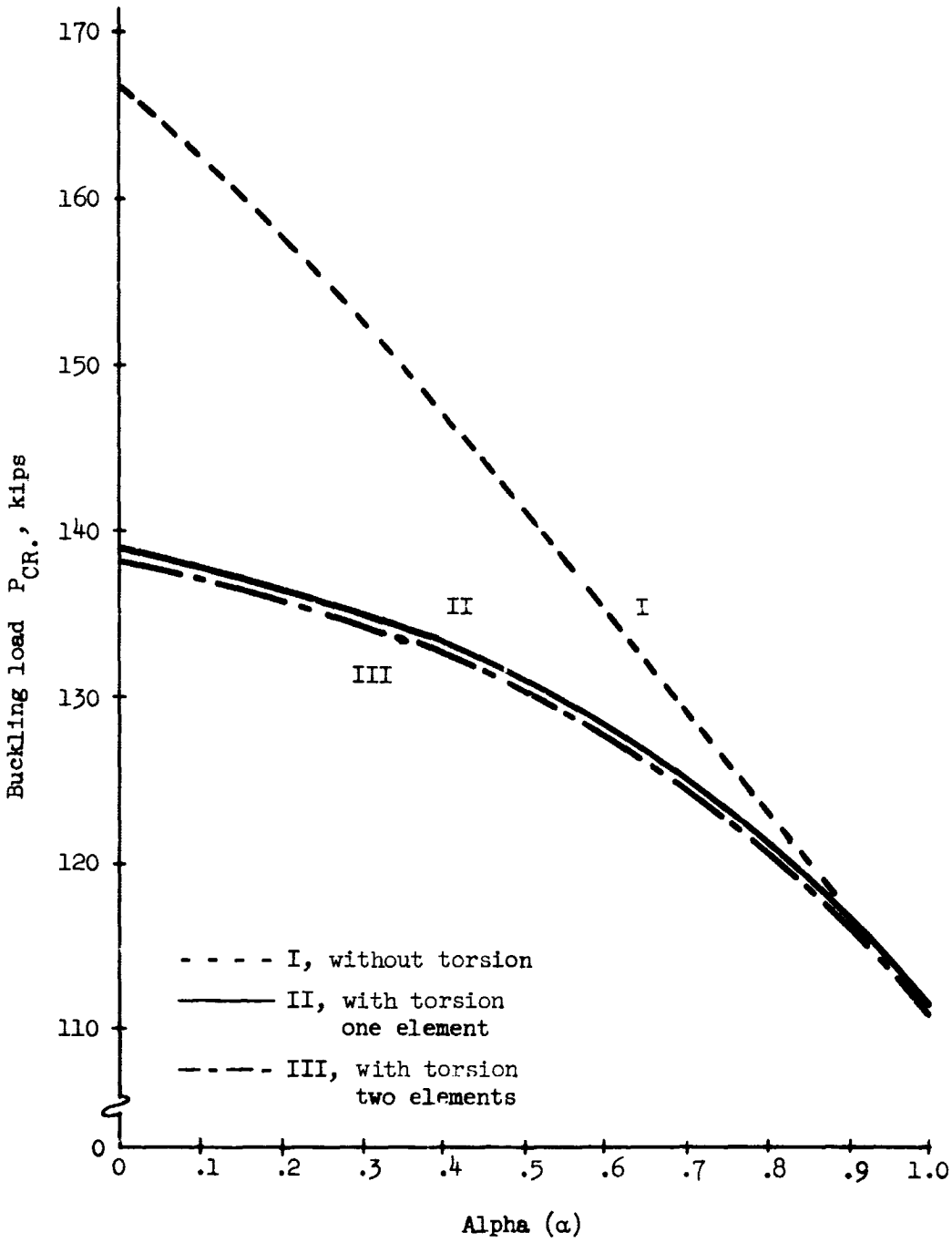

Figure 4.2.3.- Effect of load parameter (α) on $P_{CR.}$ for three-dimensional, one-bay frame.

Disp.	$\alpha = 0.0$	$\alpha = 0.5$	$\alpha = 1.0$
u_1	1.000	1.000	1.000
w_1	- .128	- .106	0
θ_{y_1}	- .252	- .195	0
θ_{x_1}	.045	.037	0
θ_{z_1}	.141	.142	.144
θ_{y_2}	- .252	.195	0
θ_{x_2}	- .045	- .037	0
θ_{z_2}	.141	.142	.144
u_3	.248	.432	1.000
w_2	.128	.106	0
θ_{y_3}	- .252	- .195	0
θ_{x_3}	.045	.037	0
θ_{z_3}	.039	.065	.144
θ_{y_4}	- .252	- .195	0
θ_{x_4}	- .045	- .037	0
θ_{z_4}	.039	.065	.144
u_{1A}	.454	.454	.456
w_{1A}	- .052	- .043	0
$\theta_{y_{1A}}$	- .126	- .097	0
$\theta_{x_{1A}}$	.086	.071	0
$\theta_{z_{1A}}$	.747	.745	.739
u_{2A}	.454	.454	.456
w_{2A}	.052	.043	0
$\theta_{y_{2A}}$	- .126	- .097	0
$\theta_{x_{2A}}$	- .086	- .071	0
$\theta_{z_{2A}}$	.747	.745	.739
u_{3A}	.114	.198	.455
w_{3A}	- .053	- .043	0

Disp.	$\alpha = 0.0$	$\alpha = 0.5$	$\alpha = 1.0$
$\theta_{y_{3A}}$	-0.126	-0.097	0
$\theta_{x_{3A}}$	.085	.071	0
$\theta_{z_{3A}}$	.176	.314	.739
u_{4A}	.114	.198	.455
w_{4A}	.053	.043	0
$\theta_{y_{4A}}$	- .126	- .097	0
$\theta_{x_{4A}}$	- .085	- .071	0
$\theta_{z_{4A}}$	.176	.314	.739
w_{1B}	0	0	0
$\theta_{y_{1B}}$	- .066	- .062	0
$\theta_{x_{1B}}$	0	0	0
$\theta_{z_{1B}}$	- .070	- .071	- .072
w_{3B}	0	0	0
$\theta_{y_{3B}}$	- .066	- .062	0
$\theta_{x_{3B}}$	0	0	0
$\theta_{z_{3B}}$	- .020	- .032	- .072
u_{3C}	.624	.716	1.000
$\theta_{z_{3C}}$	.090	.103	.144
$\theta_{y_{3C}}$	- .438	- .328	0
$\theta_{x_{3C}}$	- .022	- .019	0
u_{2C}	.624	.716	1.000
$\theta_{z_{2C}}$	.090	.103	.144
$\theta_{y_{2C}}$	- .438	- .328	0
$\theta_{x_{2C}}$	- .022	- .019	0
v_{1B}	0	0	0
v_{3B}	0	0	0
v_{3C}	0	0	0
v_{2C}	0	0	0

TABLE 4.2.4.- EIGENVECTOR COMPONENTS FOR THREE-DIMENSIONAL, ONE-BAY FRAME

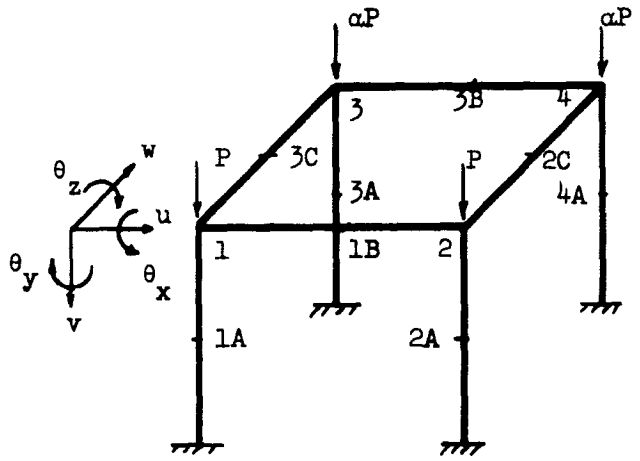

(a) Actual frame.

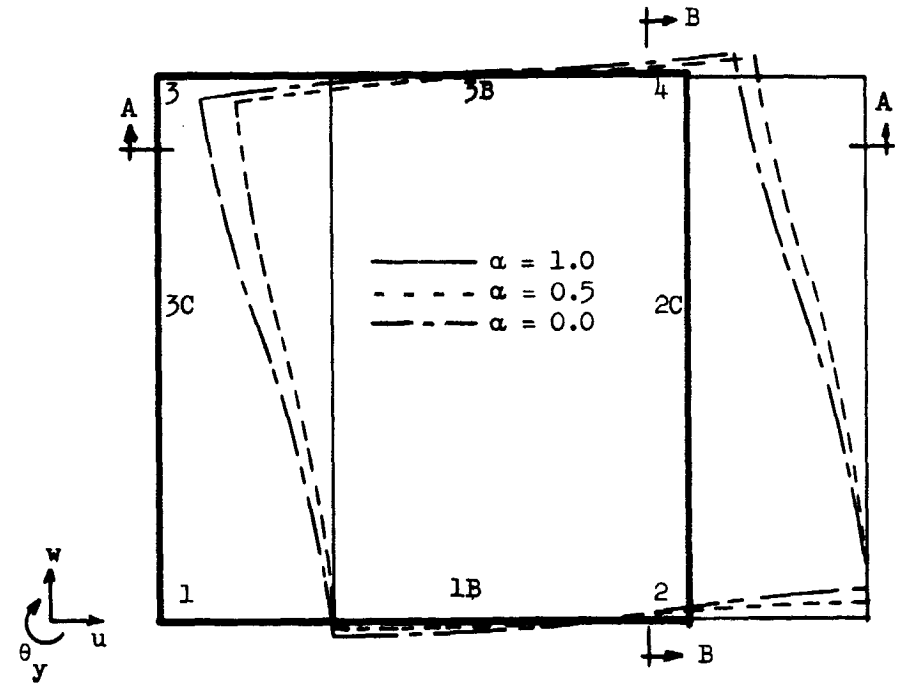

(b) Plan view.

Figure 4.2.4.- Mode shapes for three-dimensional, one-bay frame.

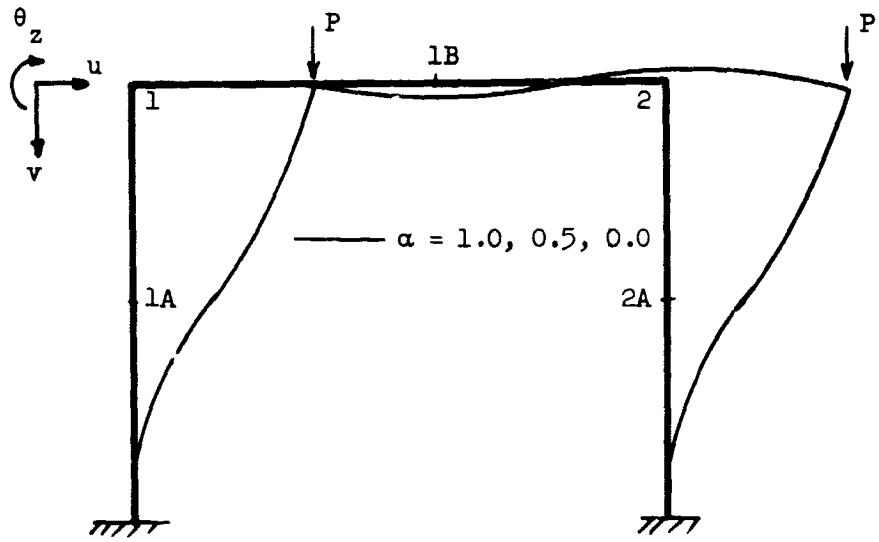

(c) Front elevation view.

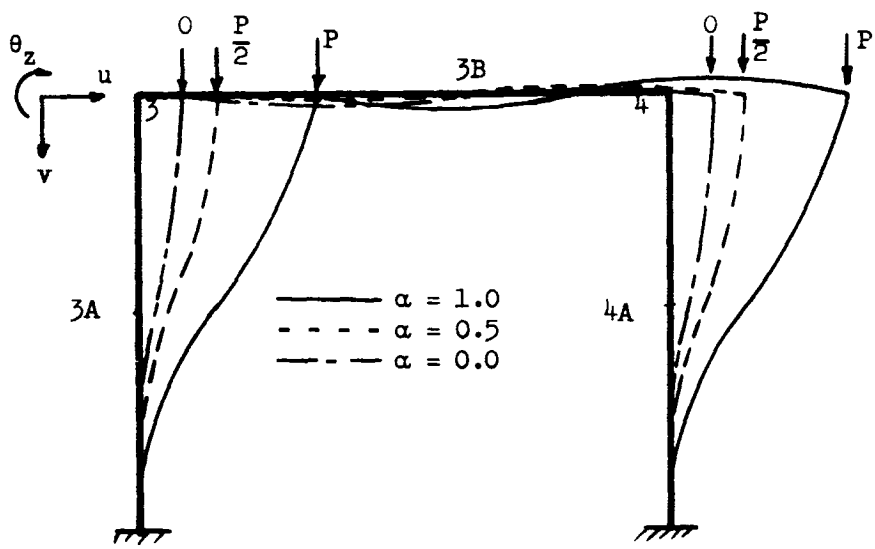

(d) Section A-A of Figure 4.2.4(b).

Figure 4.2.4.- Mode shapes for three-dimensional, one-bay frame.

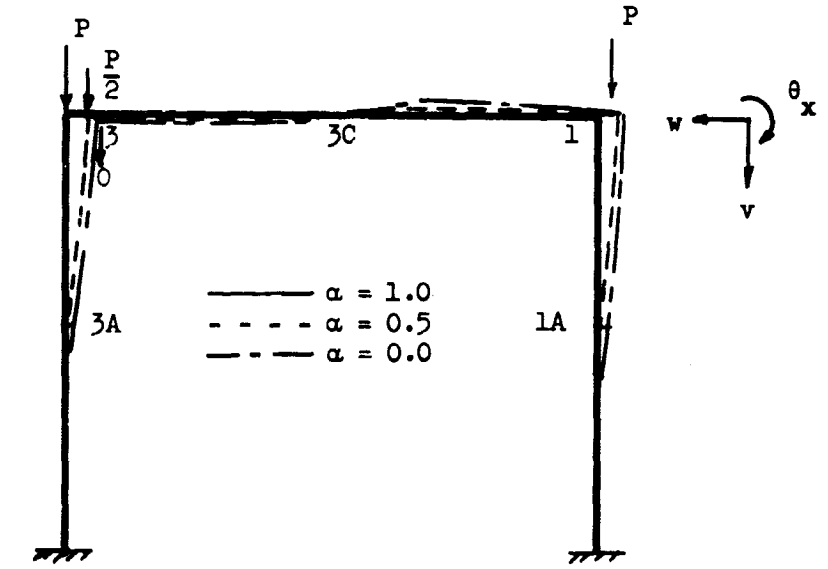

(e) Side elevation view.

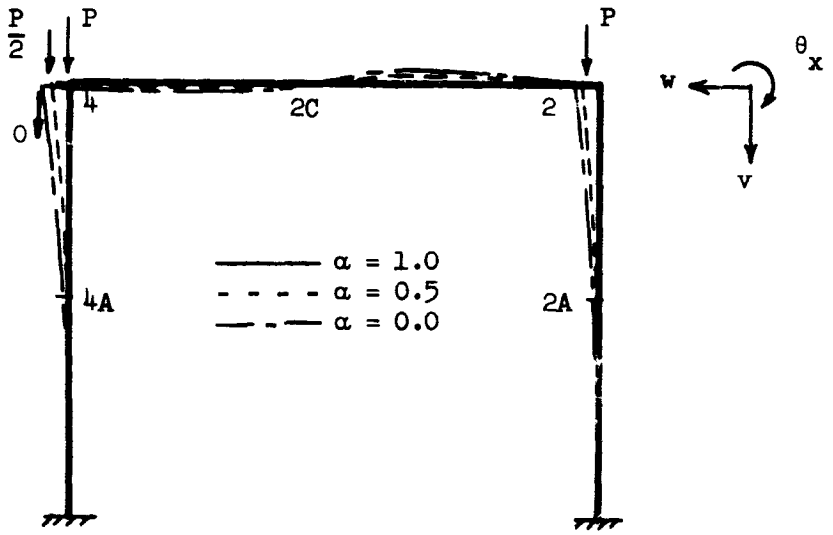

(f) Section B-B of Figure 4.2.4(b).

Figure 4.2.4.- Mode shapes for three-dimensional, one-bay frame.

4.3 Semirigid Joints

The two-dimensional rigid frame of Figure 4.2.1 (b) is used as a semirigid frame as shown in Figure 4.3.1. All of the stiffness values (R) are the same for each joint. For joints 1 and 3, the semirigid joint procedure of Chapter II as applied to Figure 2.2.1 (a) is used. This same procedure, but using Figure 2.2.1 (b) as the guide, is applied to Joint 2. The comparison of the buckling loads of Figure 4.3.1 with known values based on slope deflection procedures with fictitious members as springs[1] is shown in Table 4.3.1. The two results are plotted in Figure 4.3.2. Also shown on the plot is the range of practical moment connection stiffness obtained by Rathbun in experimental studies of joints.[5] Rathbun's tests obtained joint stiffnesses that ranged from $.001 \times 10^8 \frac{\text{in-lb.}}{\text{rad.}}$ to $4.5 \times 10^8 \frac{\text{in-lb.}}{\text{rad.}}$ for the standard AISC pinned connections and from $1.9 \times 10^8 \frac{\text{in-lb.}}{\text{rad.}}$ to $180 \times 10^8 \frac{\text{in-lb.}}{\text{rad.}}$ for moment connections.

The semirigid, three-dimensional frame, Figure 4.3.3 is developed in a similar manner as the previous frame. The results from Figure 2.2.2 (a) are used to obtain Figure 4.3.3 (R_1 to θ_z for members 1 - 2 and 3 - 4, θ_x for members 1 - 3 and 2 - 4; and R_2 to θ_y). For most connections, the relative torsional slippage at the joint will be very slight.[4] Therefore, the torsional stiffness of each member, $\left(\frac{GJ}{h}\right)$, was assumed to be constant over the member (beam or column). Therefore, torsional semirigid joints are not considered in this thesis. The buckling loads for the various values of R_1 and R_2 are computed and shown in Table 4.3.2. Using

representative values of these eigenvalues, the graphs of R_1 versus $P_{CR.}$ (Figs. 4.3.4, 4.3.5, and 4.3.6) were obtained. This is to show the upper and lower limits of each type of connection for α = 0.0, 0.5, and 1.0. Figure 4.3.7 shows the effect of α on the buckling load for various values of the joint stiffness. Also shown is the result for the joint stiffness corresponding to the weakest stiffness obtained by Rathbun in studies of typical moment connections.

Figure 4.3.8 is a sample plot of load versus determinant value at α = 0 for the three-dimensional, one-bay frame. This graph is presented to illustrate the procedure used in this paper and described in Section 4.1.

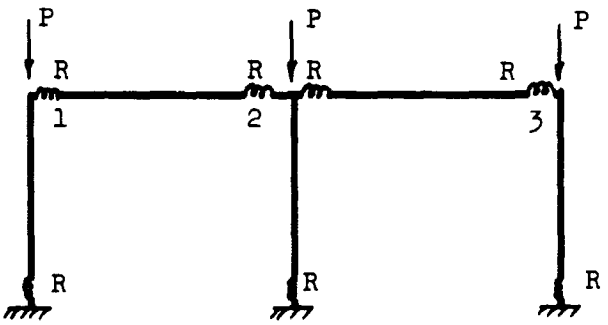

Figure 4.3.1.- Semirigid, two-dimensional, two-bay frame.

R 10^8, $\frac{\text{in-lb}}{\text{rad}}$	$P_{CR.}$, lb	
	Finite element	Slope deflection(1)
0.001	800	500
.1	47500	36600
.3	77800	66800
.8	96400	89400
1.4	102500	97700
2.1	105400	101800
3.0	107200	104500
5.0	109000	107100
10.0	110300	109100
∞	111700	111100

TABLE 4.3.1.- BUCKLING LOADS FOR SEMIRIGID, TWO-DIMENSIONAL, TWO-BAY FRAME

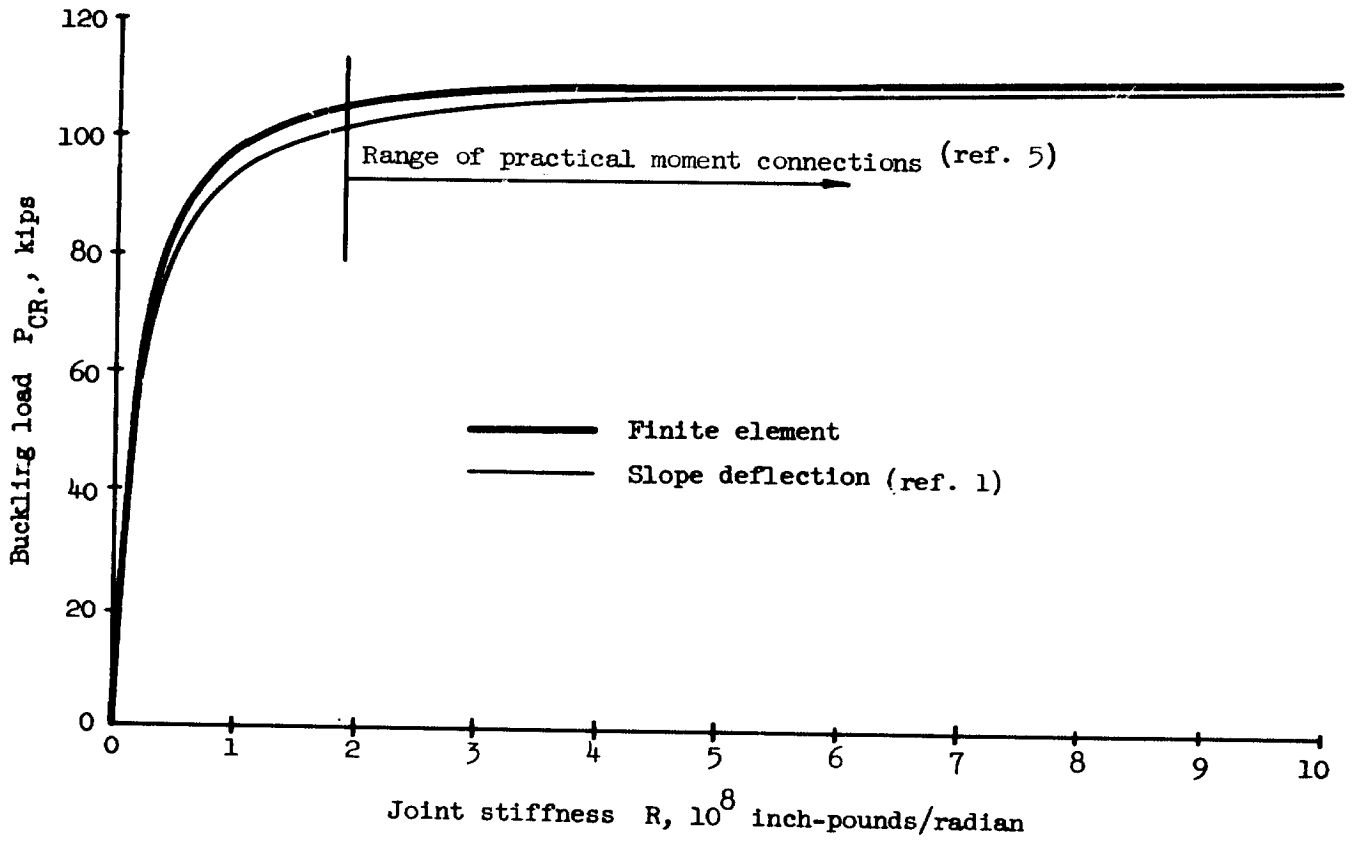

Figure 4.3.2.- Effect of semirigid joints on $P_{CR.}$ for two-dimensional, two-bay frame.

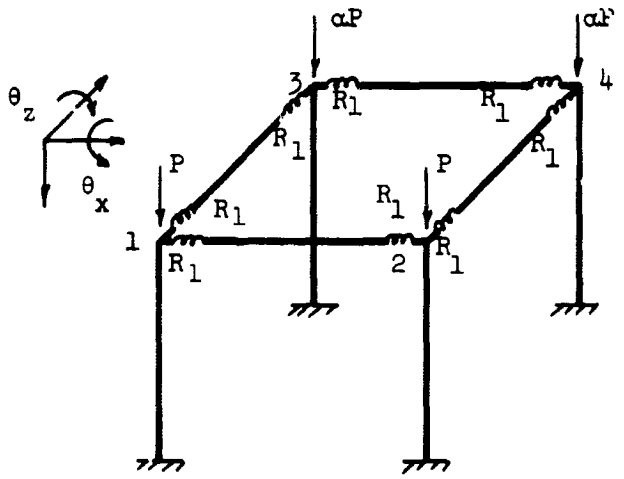

(a) Joint stiffness, R_1.

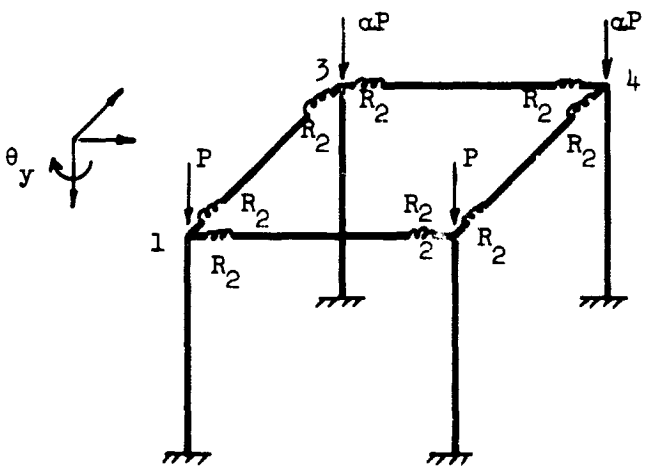

(b) Joint stiffness, R_2.

Figure 4.3.3.- Semirigid, three-dimensional, one-bay frame.

R_1 / 10^8	α	$P_{CR.}$, kips — R_2								
		1×10^5	1×10^6	5×10^6	1×10^7	1.5×10^7	5×10^7	1×10^8	1×10^9	∞
.001	0.0	32.68	34.76	39.32	41.52	42.58	44.58	45.12	45.64	45.7
	0.5	32.68	34.54	37.58	38.62	39.06	39.76	39.92	40.08	40.08
	1.0	32.24								
.1	0.0	71.06	73.44	79.56	83.04	84.92	88.7	89.78	90.88	91.0
	0.5	71.06	73.3	78.18	80.4	81.46	83.32	83.8	84.24	84.3
	1.0	70.68								
.3	0.0	91.98	94.4	101.08	105.2	107.5	112.4	113.86	115.36	115.54
	0.5	91.98	94.3	99.88	102.72	104.14	106.78	107.5	108.18	108.26
	1.0	91.6								
.8	0.0	103.18	105.62	112.54	116.96	119.5	125.1	126.8	128.58	128.88
	0.5	103.18	105.54	111.42	114.62	116.26	119.42	120.28	121.12	121.22
	1.0	102.84								
1.4	0.0	106.64	109.08	116.06	120.58	123.2	129.02	130.82	132.7	132.92
	0.5	106.64	109.0	114.98	118.28	120.0	123.34	124.26	125.16	125.26
	1.0	106.3								
2.1	0.0	108.28	110.72	117.7	122.28	124.94	130.86	132.7	134.64	134.86
	0.5	108.28	110.62	116.66	120.02	121.76	125.18	126.12	127.06	127.16
	1.0	107.94								
3.0	0.0	109.28	111.72	118.72	123.34	126.02	132.0	133.88	135.84	136.08
	0.5	109.28	111.64	117.68	121.08	122.84	126.3	127.28	128.22	128.34
	1.0	108.94								
5.0	0.0	110.24	112.66	119.7	124.34	127.04	133.1	134.98	136.98	137.22
	0.5	110.24	112.58	118.66	122.08	123.88	127.4	128.38	129.34	129.46
	1.0	109.9								
10.0	0.0	110.98	113.4	120.44	125.1	127.8	133.92	135.84	137.84	138.08
	0.5	110.98	113.32	119.42	122.86	124.66	128.22	129.22	130.2	130.32
	1.0	110.64								
100	0.0	111.64	114.06	121.12	125.78	128.52	134.68	136.6	138.64	138.88
	0.5	111.64	113.98	120.1	123.56	125.38	128.98	129.98	130.98	131.1
	1.0	111.3								

TABLE 4.3.2.- BUCKLING LOADS FOR SEMIRIGID, THREE-DIMENSIONAL, ONE-BAY FRAME

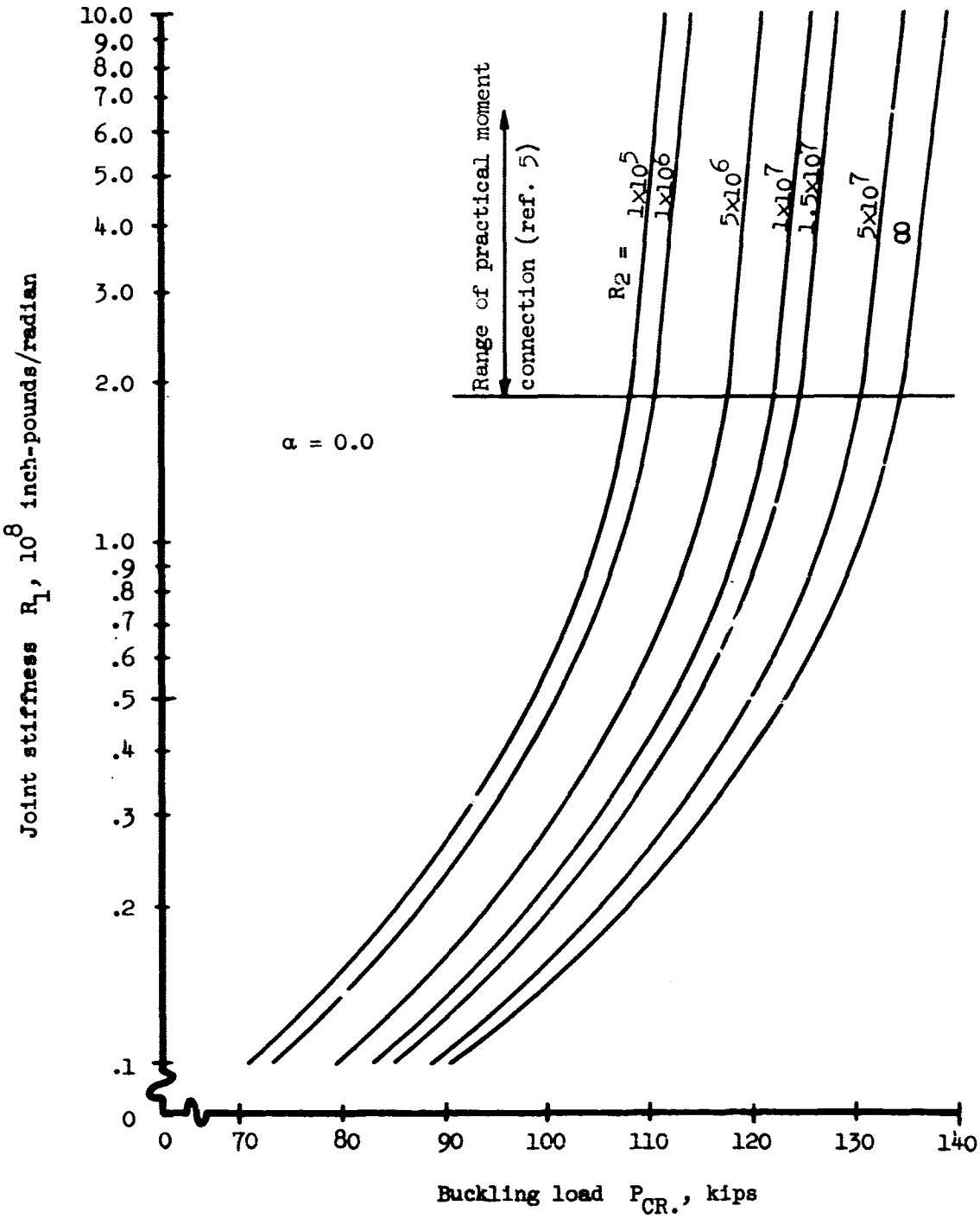

Figure 4.3.4.- Effect of semirigid joints on buckling loads of three-dimensional, one-bay frame (α = 0.0).

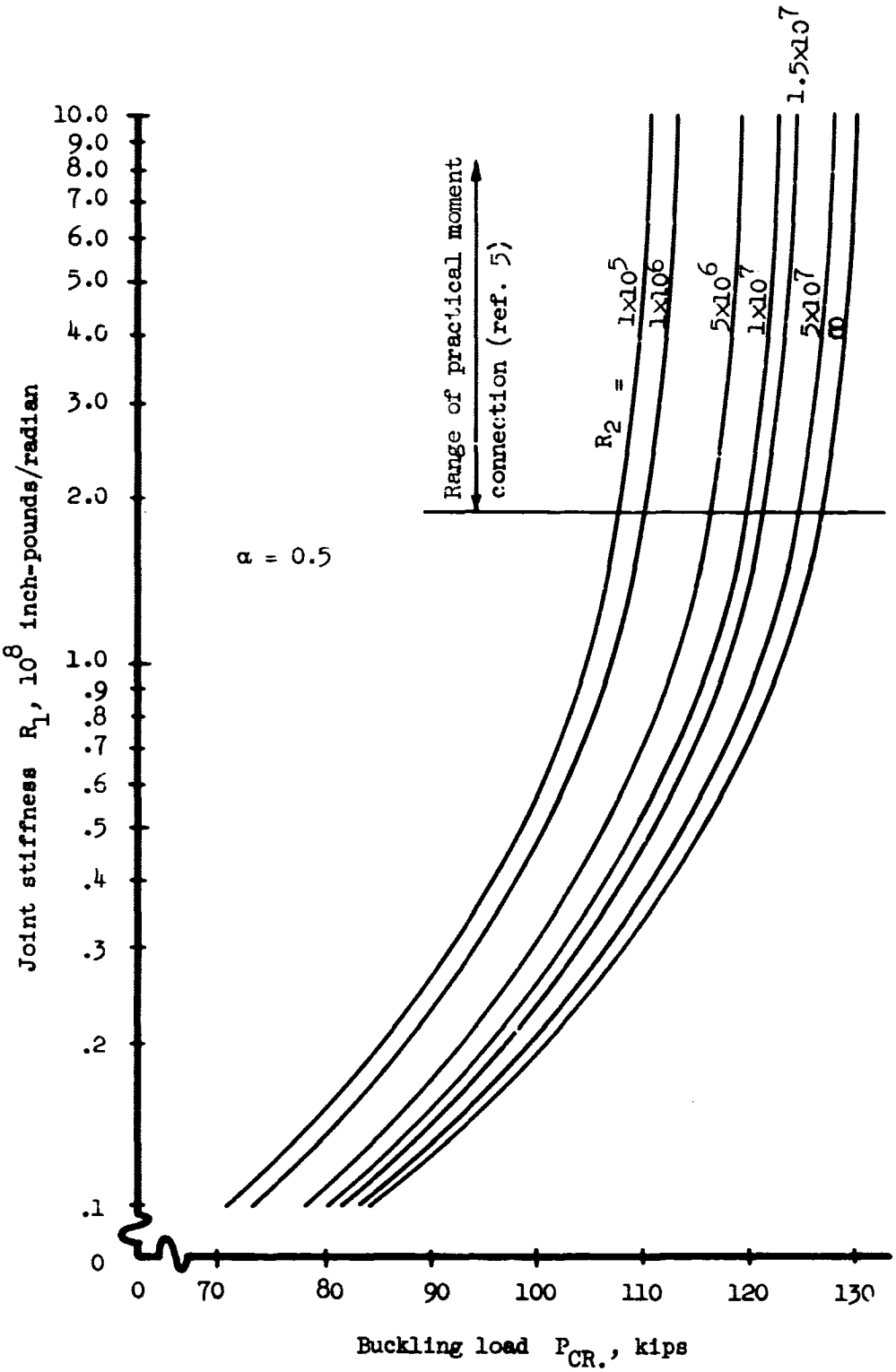

Figure 4.3.5. Effect of semirigid joints on buckling loads of three-dimensional, one-bay frames ($\alpha = 0.5$).

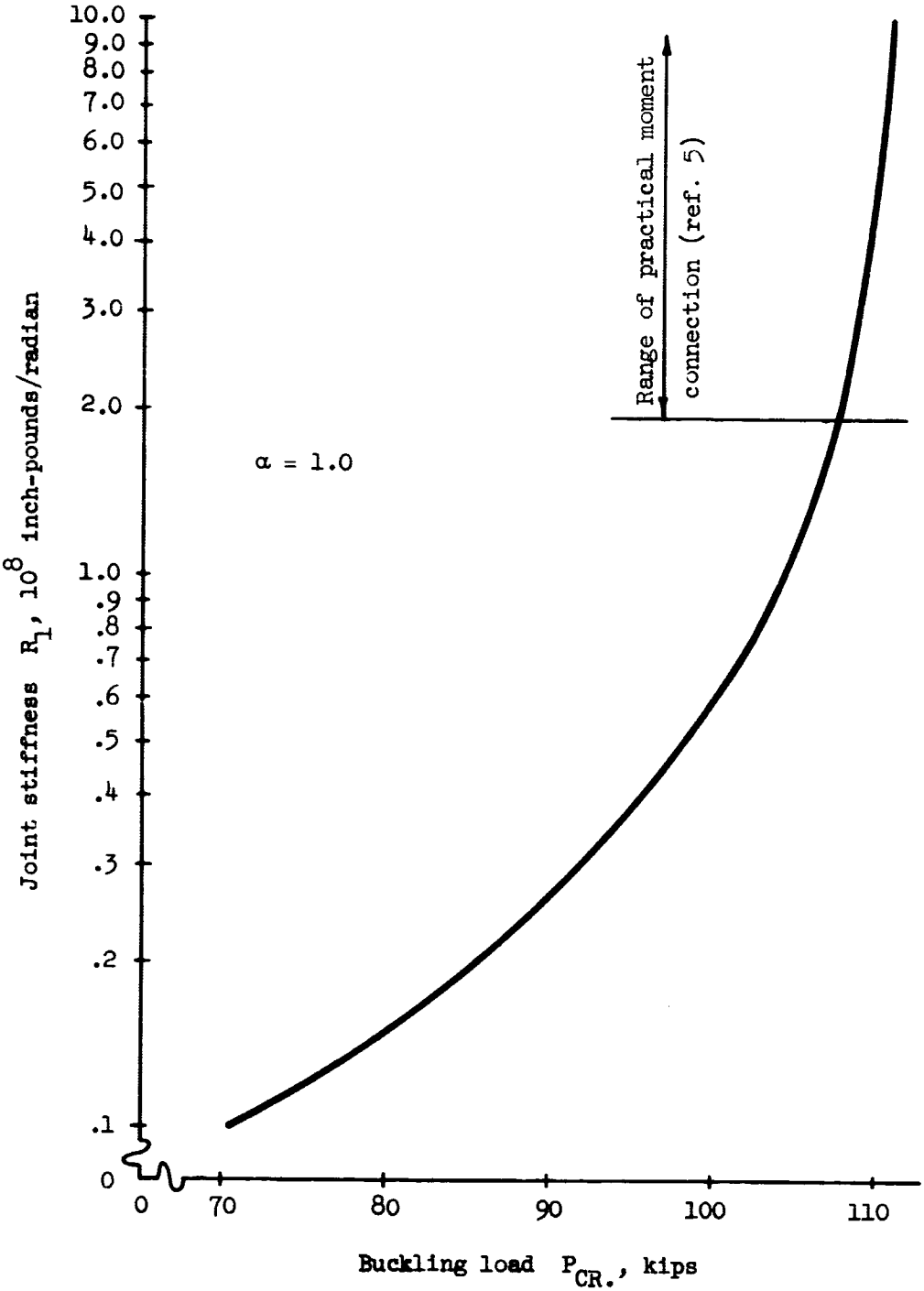

Figure 4.3.6.- Effect of semirigid joints on buckling loads of three-dimensional, one-bay frame (α= 1.0).

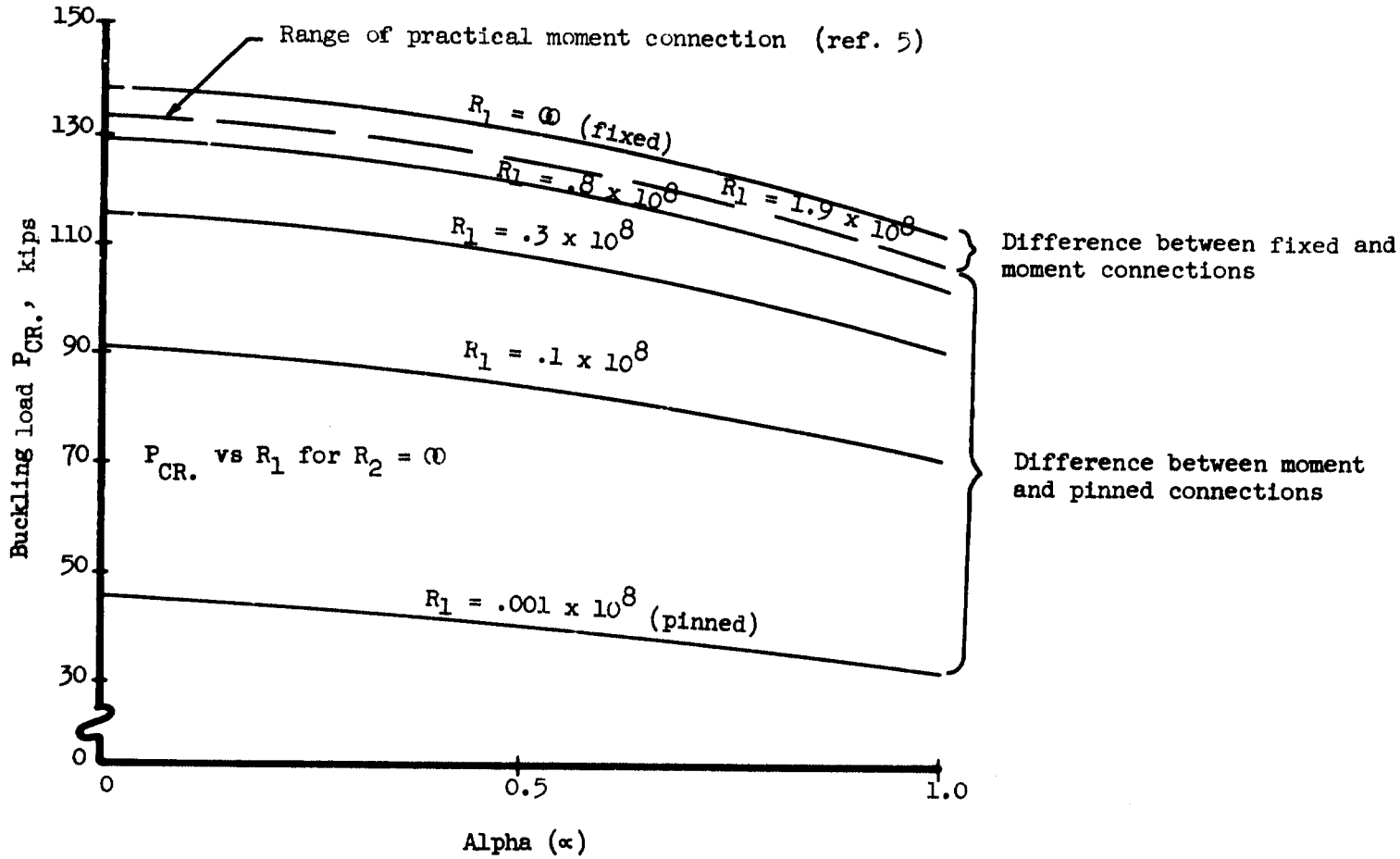

Figure 4.3.7 Effect of load parameter and semirigid joints on buckling loads for three-dimensional, one-bay frame.

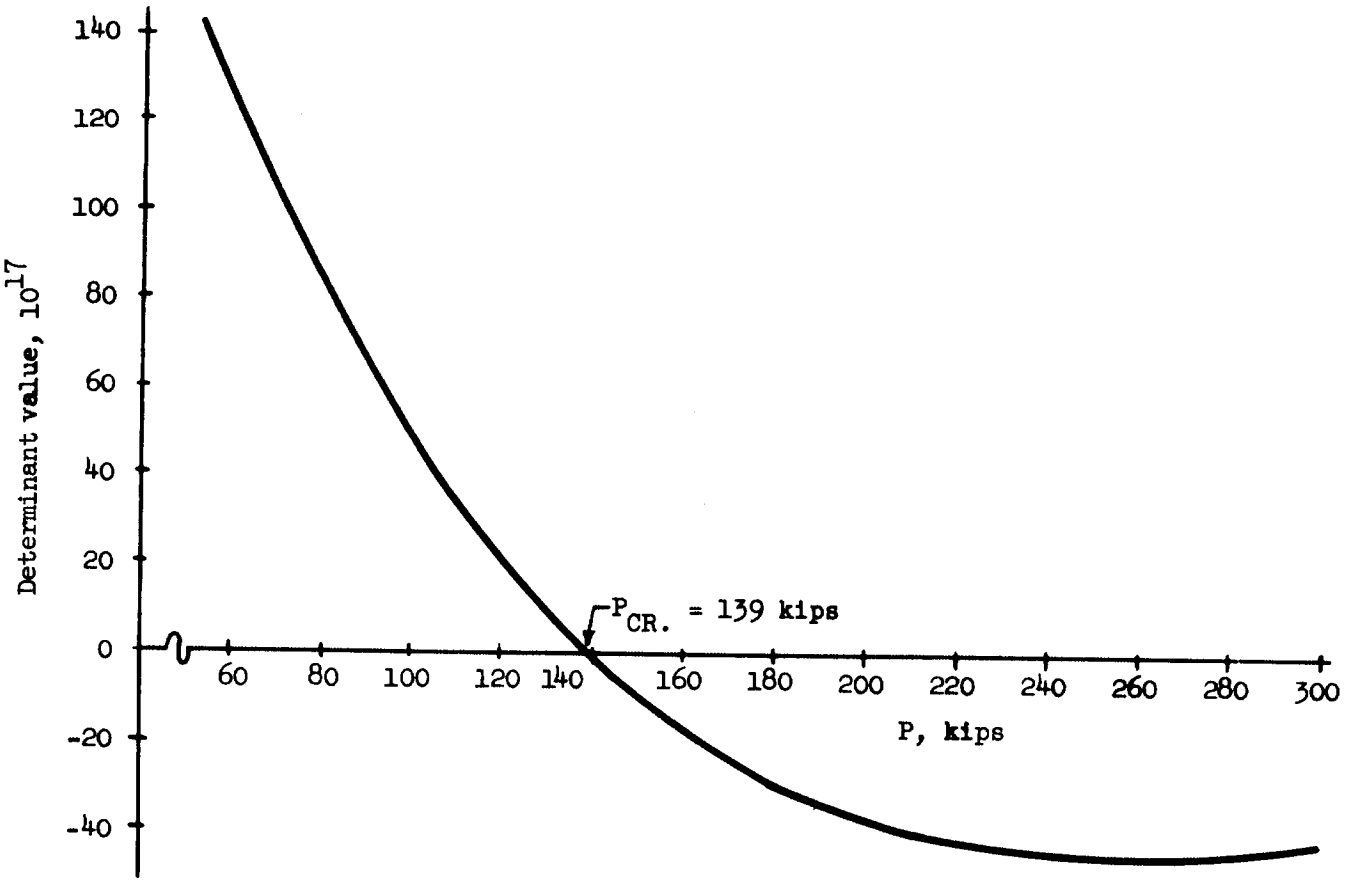

Figure 4.3.8.-Load versus determinant value at α = 0.0; three-dimensional, one-bay frame.

CHAPTER V

DISCUSSION OF RESULTS

The buckling load given in Chapter IV for the two-dimensional one-bay frame is the same as for the case when $\alpha = 1.0$ for the three-dimensional problem. The difference from the known literature value was only 1.01 per cent. Curve I of Figure 4.2.3 neglects torsional deformations in the columns and was found to be approximately a linear relationship between P and α. Curve II considers torsion and shows that the influence of torsion can reduce the buckling load by as much as 27,920 pounds or 20 per cent ($\alpha = 0.0$). Therefore, by not allowing the columns to twist, it would be possible to have a 20 per cent nonconservative estimate of the buckling load for the frame. As expected, the curves (I and II) became the same when $\alpha = 1.0$. The two-element curve (III) is shown to compliment the study of convergence in the same manner as the cantilever beam.

The two-dimensional, two-bay rigid frame was found to be the upper limiting case ($R \rightarrow \infty$) for the semirigid one. The semirigid buckling loads agree very favorably with the known values. The three-dimensional rigid frame corresponds to the upper limiting case ($\alpha = 1.0$ and $R_1 \rightarrow \infty$) for the semirigid example. Also when

α = 1.0 the same eigenvalue was obtained for $R_2 = 1 \times 10^5$ to ∞. This is due to the fact that $\theta_y = 0$ and stiffness R_2 is not necessary. Also, as expected, the semirigid buckling load curve for α = 1.0 is slightly higher than the semirigid, two-bay frame.

To develop complete reliability of the results presented, the eignevalues were checked by the following methods: (1) carefully plotting P versus determinant value (Fig. 4.3.8) to eliminate the possibility of missing the first buckling load; (2) obtaining eigenvectors to assure agreement with the assumed ones; (3) performing the check points (upper and lower limits) previously mentioned; (4) developing the study of convergence (Chapter III) to have a feel for the expected accuracy; and (5) comparing semirigid joint results with the known values.

Figures 4.3.2, 4.3.4, 4.3.5, 4.3.6, and 4.3.7 indicate that standard moment connections in both two-dimensions and three-dimensions give a close approximation to rigid joints. However, buckling loads obtained by assuming pinned connections instead of the more realistic semirigid joints considerably underestimates the buckling loads of the frames studied.

CHAPTER VI

CONCLUSIONS

A general theory for buckling of three-dimensional space frames taking into account joint flexibility has been studied. This procedure, while directed toward buckling problems, is also applicable for determining stresses and deflections of general finite element structures. This method is ideally suited to high-speed digital computation by use of a completely automated computer program.

It has been shown from the convergence study that in all cases the buckling loads will converge to the correct answer by increasing the number of finite elements. If a high degree of accuracy for calculating the eigenvalue is not needed (greater than about 1 per cent), one element is sufficient to represent the sidesway buckling behavior. By comparing the pinned column to the symmetrical buckling case, two elements are adequate for computing the buckling loads. Results on semirigidity of joints show that buckling loads will be conservative if assumed to be pinned and slightly unconservative if assumed to be rigid.

REFERENCES

LIST OF REFERENCES

1. Goering, R. S.: Buckling of Frames with Semirigid Joints. Master's thesis, VPI, May 1967, pp. 8-14, 43.

2. Lu, L. W.: A Survey of Literature on the Stability of Frames. Bulletin of the Welding Research Council, September 1962.

3. Monforton, G. R.; and Wu, T. S.: Matrix Analysis of Semi-Rigidly Connected Frames. Proceedings, ASCE, Vol. 89, No. ST6, December 1963.

4. Tezean, S. S.: Computer Analysis of Plane and Space Structures. Proceedings, ASCE, Vol. 92, April 1966, pp. 156-157.

5. Rathbun, J. C.: Elastic Properties of Riveted Connections. Transactions, ASCE, Vol. 101, 1936, pp. 524-596.

6. Martin, H. C.: Large Deflection and Stability Analysis by the Direct Stiffness Method. Technical Report No. 32-931, NASA, August 1966, pp. 1-26.

7. Langhaar, H. L.: Energy Methods in Applied Mechanics. John Wiley and Sons, Inc., New York, 1962, pp. 39-44.

8. Livesley, R. K.: Matrix Methods of Structural Analysis. The Macmillan Company, New York, 1964, pp. 92-140.

9. Fulton, Robert E.; Eppink, Richard T.; and Walz, Joseph E.: The Accuracy of Finite Elements Methods in Continuum Problems. Presented at the Fifth U.S. National Congress of Applied Mechanics, Minneapolis, Minn., June 14-17, 1966.

10. Cyrus, Nancy Jane; and Fulton, R. E.: Finite Difference Accuracy in Structural Analysis. Proceedings, ASCE Structural Division, Vol. 72, No. ST6, December 1966, pp. 459-471.

11. Cyrus, Nancy Jane; and Fulton, R. E.: Accuracy Study of Finite Difference Methods. NASA TN D-4372, January 1968.

12. Crandall, Stephen H.: Engineering Analysis. McGraw-Hill Book Company, Inc.. New York, 1956, pp. 171-173.

APPENDIX

APPENDIX

SAMPLE COMPUTER PROGRAM SHOWING THREE-DIMENSIONAL SEMIRIGID BUCKLING LOAD

```
RMF6016.                                                    LRC COMPUTER COMPLEX
JOB,1,2000,060000.        A1774,      ,2, JAMES W RAMSEY ,GMF407, MS   254 ,
```

```
                PROGRAM BUCKLG   (INPUT,OUTPUT,TAPE5=INPUT,TAPE6=OUTPUT)
000004          DIMENSION A(32,32),IM(4),LG(2),LAMB(2),IPIVOT(32),IR(5),JM(2)
000003          REAL IM,LG,IR,LR,LAMB,JM
000003          WRITE(6,1)
000007        1 FORMAT(1X,53H PLEASE SEND RESULTS TO JIM RAMSEY, MS254, PHONE 4826
                 1///1X,36H SIDESWAY BUCKLING LOAD VERSUS ALPHA)
000007          READ (5,2) (IM(I),I=1,4),(LG(I),I=1,2)
000027        2 FORMAT(6F8.1)
000027          DO 4I=1,3
000031          GO TO (5,6,7),I
000037        5 ALPHA=0.0
000040          GO TO 100
000041        6 ALPHA=0.5
000043          GO TO 100
000043        7 ALPHA=1.0
000045      100 DO 4K=1,10
000047          GO TO (30,31,32,33,34,35,36,37,38,39),K
000064       30 R=1.0E+5
000066          GO TO 14
000066       31 R=1.0E+7
000070          GO TO 14
000070       32 R=3.0E+7
000072          GO TO 14
000072       33 R=8.0E+7
000074          GO TO 14
000074       34 R=1.4E+8
000076          GO TO 14
000076       35 R=2.1E+8
000100          GO TO 14
000100       36 R=3.0E+8
000102          GO TO 14
000102       37 R=5.0E+8
000104          GO TO 14
000104       38 R=1.0E+9
000106          GO TO 14
000106       39 R=1.0E+10
000110       14 EM=30.0E+6
000112          GM=11.2E+6
000113          JM(1)=0.720
000115          JM(2)=0.540
000116          X=0.0
000117          DO 15N=1,4
```

```
000120          Y=10.0**(6-N)
000126          DO 17M=1,50
000127          DO 16J=1,32
000130          DO 16 L=1,32
000131       16 A(J,L)=0.0
000140          IR(1)=IM(2)/IM(1)
000142          IR(2)=GM*JM(1)/(EM*IM(1))
000146          IR(3)=IM(3)/IM(1)
000147          IR(4)=GM*JM(2)/(EM*IM(1))
000153          IR(5)=IM(4)/IM(1)
000155          LR=LG(2)/LG(1)
000157          C=R*LG(1)/(EM*IM(1))
000162          D=(1.0E+9)*LG(1)/(EM*IM(1))
000165          Z=M/5.0
000170          P=X+Z*Y
000173          IF (P.EQ.160000.)GO TO 4
000175          P=-P
000176          LAMB(1)=P*LG(1)**2/(30.0*EM*IM(1))
000204          LAMB(2)=ALPHA*LAMB(1)
000206          A(1,1)=24.0*(1.0+IR(3)/LR)+72.0*LAMB(1)
000214          A(1,4)=6.0*IR(3)/LR
000217          A(1,7)=-6.0-3.0*LAMB(1)
000222          A(1,11)=A(1,4)
000223          A(1,14)=A(1,7)
000225          A(1,16)=-4.0*A(1,4)
000226          A(1,18)=A(1,4)
000227          A(1,24)=A(1,7)
000230          A(2,2)=24.0*(IR(1)+IR(3)/LR)+36.0*(LAMB(1)+LAMB(2))
000241          A(2,3)=-A(1,4)
000243          A(2,5)=6.0*IR(1)+3.0*LAMB(1)
000246          A(2,9)=A(1,16)
000250          A(2,10)=A(2,3)
000251          A(2,17)=A(2,3)
000252          A(2,19)=6.0*IR(1)+3.0*LAMB(2)
000256          A(2,23)=A(2,3)
000257          A(3,2)=A(2,3)
000260          A(3,3)=4.0*IR(3)/LR+D
000264          A(3,9)=A(1,4)
000266          A(3,10)=A(1,4)/3.0
000270          A(4,1)=A(1,4)
000271          A(4,4)=4.0*IR(3)/LR+D
000274          A(4,16)=-A(1,4)
000275          A(4,18)=A(3,10)
```

```
000277          A(5,2)=A(2,5)
000300          A(5,5)=4.0*(IR(1)+LAMB(1))+C+IR(4)/LR
000307          A(5,6)=-C
000310          A(5,12)=-IR(4)/LR
000312          A(6,5)=-C
000313          A(6,6)=C+4.0*IR(5)/LR
000316          A(6,20)=2.0*IR(5)/LR
000320          A(7,1)=A(1,7)
000321          A(7,7)=A(5,5)+4.0*(1.0-IR(1))
000326          A(7,8)=-C
000327          A(7,21)=A(5,12)
000331          A(8,7)=-C
000332          A(8,8)=A(6,6)
000333          A(8,15)=A(6,20)
000335          A(9,2)=A(2,9)
000336          A(9,3)=A(1,4)
000340          A(9,9)=A(2,2)
000341          A(9,10)=A(1,4)
000342          A(9,12)=A(2,5)
000344          A(9,17)=A(1,4)
000345          A(9,23)=A(1,4)
000346          A(9,25)=A(2,19)
000347          A(10,2)=A(2,3)
000351          A(10,3)=A(3,10)
000352          A(10,9)=A(1,4)
000353          A(10,10)=A(3,3)
000355          A(11,1)=A(1,4)
000356          A(11,11)=A(4,4)
000357          A(11,16)=A(2,3)
000361          A(11,24)=A(3,10)
000362          A(12,5)=A(5,12)
000364          A(12,9)=A(2,5)
000365          A(12,12)=A(5,5)
000367          A(12,13)=-C
000370          A(13,12)=-C
000371          A(13,13)=A(6,6)
000373          A(13,26)=A(6,20)
000374          A(14,1)=A(1,7)
000376          A(14,14)=A(7,7)
000377          A(14,15)=-C
000400          A(14,27)=A(5,12)
000401          A(15,8)=A(6,20)
000402          A(15,14)=-C
```

```
000403          A(15,15)=A(6,6)
000405          A(16,1)=A(1,16)
000406          A(16,4)=-A(1,4)
000410          A(16,11)=A(2,3)
000411          A(16,16)=A(1,1)+72.0*(LAMB(2)-LAMB(1))
000416          A(16,18)=A(2,3)
000417          A(16,21)=-6.0-3.0*LAMB(2)
000422          A(16,24)=A(2,3)
000423          A(16,27)=A(16,21)
000425          A(17,2)=A(2,3)
000426          A(17,9)=A(1,4)
000427          A(17,17)=A(3,3)
000431          A(17,23)=A(3,10)
000432          A(18,1)=A(1,4)
000433          A(18,4)=A(4,18)
000435          A(18,16)=A(2,3)
000436          A(18,18)=A(4,4)
000440          A(19,2)=A(2,19)
000441          A(19,19)=A(5,5)+4.0*(LAMB(2)-LAMB(1))
000446          A(19,20)=-C
000450          A(19,25)=A(5,12)
000451          A(20,6)=A(6,20)
000453          A(20,19)=-C
000454          A(20,20)=A(6,6)
000455          A(21,7)=A(5,12)
000456          A(21,16)=A(16,21)
000460          A(21,21)=A(7,7)+4.0*(LAMB(2)-LAMB(1))
000465          A(21,22)=-C
000466          A(22,21)=-C
000467          A(22,22)=A(6,6)
000471          A(22,28)=A(6,20)
000472          A(23,2)=A(2,3)
000474          A(23,9)=A(1,4)
000475          A(23,17)=A(3,10)
000477          A(23,23)=A(3,3)
000500          A(24,1)=A(1,4)
000501          A(24,11)=A(3,10)
000502          A(24,16)=A(2,3)
000504          A(24,24)=A(4,4)
000505          A(25,9)=A(2,19)
000507          A(25,19)=A(5,12)
000510          A(25,25)=A(19,19)
000512          A(25,26)=-C
```

```
000513          A(26,13)=A(6,20)
000515          A(26,25)=-C
000516          A(26,26)=A(6,6)
000517          A(27,14)=A(5,12)
000521          A(27,16)=A(16,21)
000522          A(27,27)=A(21,21)
000524          A(27,28)=-C
000525          A(28,22)=A(6,20)
000526          A(28,27)=-C
000527          A(28,28)=A(6,6)
000531          A(3,29)=-D
000532          A(4,29)=-D
000533          A(29,3)=-D
000534          A(29,4)=-D
000535          A(29,29)=IR(2)+2.0*D
000540          A(10,30)=-D
000541          A(11,30)=-D
000542          A(30,10)=-D
000543          A(30,11)=-D
000544          A(30,30)=A(29,29)
000546          A(17,31)=-D
000547          A(18,31)=-D
000550          A(31,17)=-D
000551          A(31,18)=-D
000552          A(31,31)=A(29,29)
000553          A(23,32)=-D
000554          A(24,32)=-D
000555          A(32,23)=-D
000556          A(32,24)=-D
000557          A(32,32)=A(29,29)
000560          CALL DETEV (A,32,DETERM,IPIVOT,32,ISCALE)
000564           F(DETERM)15,4,17
000566       17 CONTINUE
000570       15 Z=X+(Z-0.20)*Y
000577          P=-X
000600        4 WRITE (6,18)P,ALPHA,R
000616       18 FORMAT (10X,F16.5,F6.2,E16.5)
000616          STOP
000620          END
```

PLEASE SEND RESULTS TO JIM RAMSEY, MS254, PHONE 4826

SIDESWAY BUCKLING LOAD VERSUS ALPHA

-4.56400E+04	0.00	1.00000E+05
-9.08800E+04	0.00	1.00000E+07
-1.15360E+05	0.00	3.00000E+07
-1.28580E+05	0.00	8.00000E+07
-1.32700E+05	0.00	1.40000E+08
-1.34640E+05	0.00	2.10000E+08
-1.35840E+05	0.00	3.00000E+08
-1.36980E+05	0.00	5.00000E+08
-1.37940E+05	0.00	1.00000E+09
-1.38640E+05	0.00	1.00000E+10
-4.00800E+04	.50	1.00000E+05
-8.42400E+04	.50	1.00000E+07
-1.08180E+05	.50	3.00000E+07
-1.21120E+05	.50	8.00000E+07
-1.25160E+05	.50	1.40000E+08
-1.27060E+05	.50	2.10000E+08
-1.28220E+05	.50	3.00000E+08
-1.29340E+05	.50	5.00000E+08
-1.30200E+05	.50	1.00000E+09
-1.30980E+05	.50	1.00000E+10
-3.22400E+04	1.00	1.00000E+05
-7.06800E+04	1.00	1.00000E+07
-9.16000E+04	1.00	3.00000E+07
-1.02840E+05	1.00	8.00000E+07
-1.06300E+05	1.00	1.40000E+08
-1.07940E+05	1.00	2.10000E+08
-1.08940E+05	1.00	3.00000E+08
-1.09900E+05	1.00	5.00000E+08
-1.10640E+05	1.00	1.00000E+09
-1.11300E+05	1.00	1.00000E+10

```
02/19/68  LRC SCOPE 3.0       6600C-131K  02/12/68
14.26.50.RMF6016.
14.26.50.                     LRC COMPUTER COMPLEX
14.26.50.JOB,1,2000,060000.        A1774,     ,2,
14.26.50. JAMES W RAMSEY ,GMF407, MS   254 ,
14.26.51.RUN(S)
14.26.58.SETINDF.
14.26.59.LGO.
14.37.15.STOP
14.37.15.CPU    385.822971 SEC.
14.37.15.PPU    006.159488 SEC.
  RMF6016. PRINT-PP 00365 LINES
```